

การศึกษาเชิงทฤษฎีของการเกิดแสงเช้คกันฮาร์โมนิกตามแนวระต้อนจาก

ผลึกรูปเตียมไดไฮโดรเจนฟอสเฟต

นางสาวมัญญกรณ วังศ์คำดี

วิทยานิพนธ์นี้เป็นส่วนหนึ่งของการศึกษาหลักสูตรปริญญาวิทยาศาสตรมหาบัณพิต

สาขาวิชาเทคโนโลยีเลเซอร์และโฟตอนิกส์

มหาวิทยาลัยเทคโนโลยีสุรนารี

ปีการศึกษา 2543

ISBN 974-7359-62-6

**THEORETICAL STUDY OF REFLECTED SECOND  
HARMONIC GENERATION IN RUBIDIUM  
DIHYDROGEN PHOSPHATE (RDP) CRYSTAL**

**Miss Manunporn Wongkumdee**

**A Thesis Submitted in Partial Fulfillment of the Requirements for the Degree of**

**Master of Science in Laser Technology and Photonics**

**Suranaree University of Technology**

**Academic Year 2000**

**ISBN 974-7359-62-6**

**Thesis Title**

**Theoretical study of reflected second harmonic generation  
in rubidium dihydrogen phosphate (RDP) crystal**

Suranaree University of Technology Council has approved his thesis  
submitted in partial fulfillment of the requirements for a Master's Degree

Thesis Examining Committee

.....  
(Prof. Dr. Vutthi Bhanthumnavin)  
Chairman

.....  
(Prof. Dr. Vutthi Bhanthumnavin)  
Thesis Advisor

.....  
(Asst. Prof. Dr. Joewono Widjaja)  
Member

.....  
(Asst. Prof. Dr. Arjuna Chaiyasena)  
Member

.....  
(Assoc. Prof. Dr. Kasem Prabripataloong)  
Vice Rector for Academic Affairs

.....  
(Assoc. Prof. Dr. Tassanee Sukosol)  
Dean / Institute of Science

นางสาวมัญญกรณ์ วงศ์คำดี: การศึกษาเชิงทฤษฎีของการเกิดแสงเช็คกันฮาร์โมนิกตามแนวสะท้อน  
จากผลึกยูบิเดียมไดไฮโดรเจนฟอสเฟต (THEORETICAL STUDY OF REFLECTED  
SECOND HARMONIC GENERATION IN RUBIDIUM DIHYDROGEN  
PHOSPHATE (RDP) CRYSTAL อ. ที่ปรึกษา : ศ. ดร. วุฑฒิ พันธุมนาวิน, 103 หน้า ISBN  
974-7359-62-6

การศึกษาการเกิดแสงเช็คกันฮาร์โมนิกในแนวสะท้อนจากผลึกยูบิเดียมไดไฮโดรเจน  
ฟอสเฟตซึ่งมีอนลิเนียร์โพราไรเซชัน  $\bar{P}_{2\omega}^{NLS}$  วางตัวในแนว [001] และทำมุม  $\beta$  กับพื้นผิวตก  
กระทบต่าง ๆ กันกระทำโดยให้ผลึกวางตัวในของเหลว 1-โบรโมเนปทาไลน์ที่มีค่าดัชนีสูงกว่า โดย  
ใช้แสงเลเซอร์ที่มีช่วงพัลส์แคบมากและมีโพราไรเซชันในแนว  $[1\bar{1}0]$  เป็นลำแสงตกกระทบ ผล  
การคำนวณพบว่าภายใต้เงื่อนไขของเฟสแมช ซึ่ง  $\beta = \theta_m = 52.93^\circ$  ทำให้เกิดความเข้มของแสง  
เช็คกันฮาร์โมนิกสูงสุดที่มุมตกกระทบวิกฤต  $\theta_i = 66.67^\circ$  และพบว่าเกิดมมอนลิเนียร์บริวเตอร์  
 $\theta_i^{NB} = 33.30^\circ$  นอกจากนี้ได้พบว่าที่มุมตกกระทบวิกฤตเกิดความเข้มของแสงเช็คกันฮาร์โมนิก  
ในแนวสะท้อนต่ำสุดซึ่งเป็นเงื่อนไขของมมอนลิเนียร์บริวเตอร์ที่  $\beta = 0^\circ$  และเมื่อกำหนดค่า  
 $\beta = 90^\circ$  และ  $56.77^\circ$  จะเกิดมมอนลิเนียร์บริวเตอร์ที่  $0^\circ$  และ  $30^\circ$  ตามลำดับ

สาขาวิชาเทคโนโลยีเลเซอร์  
และโฟตอนิกส์  
ปีการศึกษา 2543

ลายมือชื่อนักศึกษา.....  
ลายมือชื่ออาจารย์ที่ปรึกษา.....  
ลายมือชื่ออาจารย์ที่ปรึกษาร่วม.....  
ลายมือชื่ออาจารย์ที่ปรึกษาร่วม.....

**MANUNPORN WONGKUMDEE: THEORETICAL STUDY OF REFLECTED SECOND HARMONIC GENERATION IN RUBIDIUM DIHYDROGEN PHOSPHATE (RDP) CRYSTAL THESIS ADVISOR: PROF. VUTTHI BHANTHUMNAVIN, Ph. D. 103 PP. ISBN 974-7359-62-6**

Theoretical calculation for reflected second harmonic intensity (SHI) is performed in RDP crystal having nonlinear polarization,  $\vec{P}_{2\omega}^{NLS}$ , in [001] direction. The investigation of reflected SHI as a function of incident angle is demonstrated by means of varying an angle  $\beta$  with incident surface of crystal, which is immersed in optically denser fluid, 1-Bromonaphthalene. The ultrashort pulsed laser of 900 nm with the polarization in  $[1\bar{1}0]$  direction is utilized as the excitation source. According to the calculation under phase matched condition at the reflection, the maximum reflected SHI is achieved at  $\theta_i = \theta_{\omega}^{cr} = 66.67^\circ$ , and also the minimum value of SHI occurs at a nonlinear Brewster angle,  $\theta_i^{NB} = 33.30^\circ$  with  $\beta = \theta_m = 52.93^\circ$ . However, the minimum of reflected SHI clearly occurs at this critical angle,  $\theta_i^{NB} = \theta_{\omega}^{cr}$  when  $\beta = 0^\circ$ . In addition, when  $\beta = 90^\circ$  and  $56.77^\circ$  the minimum reflected SHI are at  $\theta_i^{NB} = 0^\circ$  and  $30^\circ$ , respectively.

สาขาวิชาเทคโนโลยีเลเซอร์  
และโฟตอนิกส์  
ปีการศึกษา 2543

ลายมือชื่อนักศึกษา.....  
ลายมือชื่ออาจารย์ที่ปรึกษา.....  
ลายมือชื่ออาจารย์ที่ปรึกษาร่วม.....  
ลายมือชื่ออาจารย์ที่ปรึกษาร่วม.....

## **ACKNOWLEDGEMENTS**

I am indebted to my father and mother for their devotion and inspiring me at all times in Science and Technology. Their efforts are beyond evaluation. I would like to express my gratitude to my family and relatives who have kindly supplied me every supported encouraged me all along. I would like to express my deeply sincere thanks to Prof. Dr. Vutthi Bhanthumnavin for his advice, help, access to a computing facility, reading and correction of my manuscript. I also particularly want to thank Asst. Prof. Dr. JoEwono Widjaja and Asst. Prof. Dr. Arjuna Chaisena who taught me fundamental graduate courses and offer suggestions me for improving my thesis, as well as Assoc. Prof. Dr. Prapasri Adsavakul and Asst. Prof. Dr. Eckart Schulz kindly provided very useful advice during my teaching assistantship. Furthermore, I am very grateful for Sutthitheps' family who warmly supplied me with an efficient computer. Helps and suggestions were supplied by, my colleagues, Miss Ubol Suripol and Mr. Songrit Kamyod. The greatly and sincere appreciation are referred to my friend Mr. Sathidchoke Phosa-ade, Miss Naruemol Thummageard and Mr. Charat Jeravipoolvarn for their helps and suggestion about computer program. And I also thank Mrs. Rapeephaen Srichy for her generous attention. I am also in debt to my all teachers whose devotion, teaching, advice and etc that help to shaped me up to present are invaluable. Finally, with all generous assistant and careful guided and sincere advice and etc from all persons mentioned above, I am able to complete Master Degree within 4 trimesters.

Manunporn Wongkumdee

# CONTENTS

	<b>Page</b>
<b>Abstract (Thai)</b> .....	<b>I</b>
<b>Abstract (English)</b> .....	<b>II</b>
<b>Acknowledgements</b> .....	<b>III</b>
<b>Contents</b> .....	<b>IV</b>
<b>Lists of Tables</b> .....	<b>VIII</b>
<b>Lists of Figures</b> .....	<b>IX</b>
<b>Lists of Symbols</b> .....	<b>XII</b>
<b>Chapter I: Introduction</b> .....	<b>1</b>
1.1 Literature Review.....	1
1.2 Research Objective.....	4
1.3 Research Hypothesis.....	4
1.4 Scope and Limitations of the Study.....	4
<b>Chapter II: Theory</b> .....	<b>6</b>
2.1 Polarization in an Anisotropic Crystal.....	6
2.1.1 Uniaxial Crystal and Its Index of Ellipsoid.....	7
2.1.2 Physical Origin of Polarization in Isotropic and Anisotropic Media.....	9
2.1.2.1 Linear Polarization.....	10
2.1.2.2 Nonlinear Polarization.....	12

## CONTENTS (CONTINUED)

	<b>Page</b>
2.2 Second Harmonic Generation in Reflection.....	19
2.2.1 Second Harmonic Waves Emanating from a Boundary.....	19
2.2.2 Generalized Snell's Law.....	23
2.2.3 Polarization in Plane of Incidence and Second Harmonic Intensity in Reflection.....	26
2.3 Phase Matching in Second Harmonic Generation.....	36
2.4 Nonlinear Brewster Angle, $\mathbf{q}_i^{NB}$ .....	39
<b>Chapter III: Procedure.....</b>	<b>41</b>
3.1 Ultrashort Pulse Laser.....	41
3.2 Rubidium Dihydrogen Phosphate (RDP) Crystal.....	42
3.3 Liquid 1-Bromonaphthalene.....	44
3.4 Computer Program.....	45
<b>Chapter IV: Results and Discussion.....</b>	<b>48</b>
4.1 Phase Matched at Total Reflection.....	48
4.1.1 Phase Matched SHI at Total Reflection.....	49
4.1.2 Nonlinear Brewster Angle at $\mathbf{q}_i = \mathbf{q}_i^{NB} = 33.30^\circ$ .....	51
4.2 Nonlinear Brewster Angles.....	52
4.2.1 Nonlinear Brewster Angle at $\mathbf{q}_i = \mathbf{q}_i^{NB} = 0^\circ$ .....	53

## CONTENTS (CONTINUED)

	<b>Page</b>
4.2.2 Nonlinear Brewster Angle at $\mathbf{q}_i = \mathbf{q}_i^{NB} = \mathbf{q}_{2w}^{cr} = 68.14^\circ$ .....	55
4.3 Investigation for a Definite Orientation of $\vec{P}_{2w}^{NLS}$ when $\mathbf{q}_i^{NL} = 30^\circ$ is Specified.....	57
<b>Chapter V: Discussion and Conclusions</b> .....	61
<b>References</b> .....	68
<b>Appendixes</b> .....	71
Appendix A: The Calculation for Refractive Indices.....	72
A.1 The Calculation for Indices of Refraction of RDP Crystal.....	72
A.2 The Calculation for Indices of Refraction of 1-Bromonaphthalene .....	74
Appendix B: The Existence of Nonlinear Brewster Angle, $\mathbf{q}_i^{NB}$ , by Setting the Angle between a Crystal Surface and Nonlinear Polarization, $\mathbf{b}$ .....	77
Appendix C: Computer Program (C++).....	83
C.1 Reflected SHI of RDP Crystal at 900 nm with Nonlinear Polarization 52.93 degrees lies with face normal.....	83

**CONTENTS (CONTINUED)**

	<b>Page</b>
C.2 Reflected SHI of RDP Crystal at 900 nm with Nonlinear Polarization lies in face normal.....	88
C.3 Reflected SHI of RDP Crystal at 900 nm with Nonlinear Polarization 90 degree lies with face normal.....	92
C.4 Reflected SHI of RDP Crystal at 900 nm with Nonlinear Polarization 56.77 degree lies with face normal.....	97
<b>Biography.....</b>	<b>103</b>

## LISTS OF TABLES

Table	Page
5.1	Summary of nonlinear Brewster angles corresponding to various orientation of $\vec{P}_{2w}^{NLS}$ .....62
A.1	Changes in refractive indices of RDP crystal with a wavelength range 0.266-1.064 $\mu\text{m}$ .....73
A.2	Changes in refractive indices of 1-Bromonaphthalene with a wavelength range 0.434-1.064 $\mu\text{m}$ .....75
A.3	The sets of samples and calculated RDP refractive indices and its average value.....76

## LISTS OF FIGURES

Figure	Page
2.1	Reflective Index of (a) a negative (b) a positive uniaxial crystal.....8
2.2	The intersection of $\vec{k}$ and the surface of ellipsoid is indicated for $n_e(\mathbf{q})$ .....9
2.3	Symmetrical potential energy in linear medium.....10
2.4	Asymmetrical potential energy in nonlinear medium.....12
2.5	Relation between induced polarization and the electric field causing it in (a) a symmetrical and (b) asymmetric crystal.....14
2.6	An applied sinusoid electric field and the resulting polarization in (a) symmetric and (b) asymmetric crystal.....15
2.7	Analysis of the nonlinear polarization wave (a) of figure 2.6 (b) shown that it contains components oscillation at (b) the same frequency ( $\omega$ ) as the wave inducing it, (c) twice that frequency ( $2\omega$ ) and (d) an average (dc) negative component.....16
2.8	The incident, reflected and transmitted rays at the fundamental and second harmonic frequencies near the boundary between a RDP crystal and linear medium.....22

## LISTS OF FIGURES (CONTINUED)

Figure	Page
2.9	Two incident rays at frequencies $\omega_1$ and $\omega_2$ create a reflected wave, a homogeneous transmitted wave at the sum frequency $\omega_3 = \omega_1 + \omega_2$ , all emanating from the boundary between the linear and nonlinear medium....23
2.10	The harmonic wave at the boundary of a nonlinear medium with electric field vector in the plane of refraction. Both the nonlinear polarization and the electric field may have longitudinal components.....28
2.11	The propagated direction of harmonic wave at the boundary of RDP crystal and 1-Bromonaphthalene liquid.....33
2.12	The geometry of the RDP refractive index of ellipsoid employed to investigate the reflected SHI.....34
2.13	Geometry for phase matching in negative uniaxial crystal.....38
2.14	Geometry for existing nonlinear Brewster angle.....39
3.1	The flowchart for theoretical calculation of reflected second harmonic Intensity.....47
4.1	The reflected second harmonic intensity with the nonlinear polarization making the angle $52.93^\circ$ to the incident surface of RDP crystal, $I_{2\omega}^R$ is minimum at $\mathbf{q}_i^{NB} = 33.30^\circ$ and $I_{2\omega}^R$ is maximum at $\mathbf{q}_i = \mathbf{q}_w^{cr} = 66.67^\circ$ .....50

**LISTS OF FIGURES (CONTINUED)**

<b>Figure</b>	<b>Page</b>
4.2 The reflected second harmonic intensity with the nonlinear polarization lies along face normal. Nonlinear Brewster angle $\mathbf{q}_i^{NB} = 0^\circ$ .....	54
4.3 The reflected second harmonic intensity with the nonlinear polarization along the incident surface of RDP crystal. Nonlinear Brewster angle $\mathbf{q}_i^{NB} = \mathbf{q}_w^{cr} = 68.14^\circ$ .....	56
4.4 The reflected second harmonic intensity with the nonlinear polarization is at $\mathbf{b} = 56.77^\circ$ with respect to the incident surface. Nonlinear Brewster angle $\mathbf{q}_i^{NB} = 30^\circ$ .....	59
B.1 The orientation of $\vec{P}_{2w}^{NLS}$ causes $\mathbf{q}_i^{NB} = 30^\circ$ .....	77

## LISTS OF SYMBOLS

$\vec{P}$	=	Total Polarization
$\vec{P}^L$	=	Linear Polarization
$\vec{P}^{NLS}$	=	Nonlinear Polarization
$n_o$	=	Ordinary Ray Index
$n_e$	=	Extraordinary Ray Index
$n_o^{2w}$	=	Refractive Index of Transmitted Homogeneous Wave Vector
$n_e^{2w}$	=	Refractive Index of Transmitted Source Wave Vector
nm	=	nanometer
$\mathbf{c}^L$	=	Linear Polarization
$\mathbf{c}^{NL}$	=	Nonlinear Polarization
$\mathbf{w}$	=	Frequency
$\mathbf{e}$	=	Permittivity of Crystal
$\mathbf{m}$	=	Permeability of Crystal
$\vec{D}$	=	Electric Flux Density
$\vec{J}$	=	Electric Current Density
$\mathbf{r}$	=	Electric Charge Density
$\vec{B}$	=	Magnetic Flux Density
$\vec{H}$	=	Magnetic Field

## LISTS OF SYMBOLS (CONTINUED)

$\nabla^2$	=	Laplacian Operator
$c$	=	Speed of Light being $3 \times 10^8$ m/s
$t$	=	time
$\vec{E}$	=	Electric Field
$\vec{E}_w^T$	=	Transmitted Electric Field in Crystal
$\vec{k}_w^i$	=	Incident Wave Vector at Fundamental Frequency
$\vec{k}_w^r$	=	Reflected Wave Vector at Fundamental Frequency
$\vec{k}_w^t$	=	Transmitted Wave Vector at Fundamental Frequency
$\vec{k}_{2w}^R$	=	Reflected Wave Vector at Second Harmonic Frequency
$\vec{k}_{2w}^S$	=	Transmitted Wave Vector at Fundamental Frequency
$\vec{k}_{2w}^T$	=	Transmitted Wave Vector at Second Harmonic Frequency
$\vec{E}_{2w}^R$	=	Electric Field of Reflected Second Harmonic Light
$\vec{E}_{2w}^T$	=	Electric Field of Transmitted Second Harmonic Light
$\vec{H}_{2w}^R$	=	Magnetic Field of Reflected Second Harmonic Light
$\vec{H}_{2w}^T$	=	Magnetic Field of Transmitted Second Harmonic Light
$E_{2w}^R$	=	Amplitude of Electric Field of Reflected Second Harmonic Light
$E_{2w}^T$	=	Amplitude of Electric Field of Transmitted Second Harmonic Light

**LISTS OF SYMBOLS (CONTINUED)**

$\vec{P}_{\perp}^{NLS}$	=	Nonlinear Polarization Perpendicular to Plane of Incidence
$\vec{P}_{//}^{NLS}$	=	Nonlinear Polarization Parallel to Plane of Incidence
$F_{T,\perp}^L$	=	Linear Fresnel Factor of Transmitted Wave Perpendicular to Plane of Incidence
$F_{R,//}^{NL}$	=	Nonlinear Fresnel Factor of Reflected Wave Parallel to Plane of Incidence
$I_{2w}^R$	=	Intensity of Reflected Second Harmonic Generation
$A_R$	=	Cross Section Area of Reflected Second Harmonic Generation

# CHAPTER I

## INTRODUCTION

### 1.1 Literature Review

After the advent of LASER or Light Amplification by Stimulated Emission Radiation by Maiman (1960) using ruby as the laser medium at Hughes Aircraft Co. laboratory, the ruby optical maser at wavelength  $\lambda = 694.3$  nm was utilized as the coherent source, making possible the experimental observation of nonlinear effects, especially second harmonic generation (SHG). The first nonlinear optical experiment was performed by Franken, Hill, Peter, and Weinrich (1961). In their experiment, the observable second harmonic intensity (SHI) in transmission was the unambiguous blue light at  $\lambda = 347.15$  nm when the pulsed ruby laser was focused through a quartz plate as the nonlinear material. In their experiment, it was also found that the light at the wavelength of 347.15 nm exhibited the expected dependence on polarization orientation. Later Maker, Terhune, Nisenoff, and Savage and independently Geordmaine (1962) performed an SHG experiment, which successfully enhanced the higher SHI in transmission by the phase matching technique. Furthermore, Bloembergen and Pershan (1962) theoretically analyzed the behavior of light waves at the boundary of a nonlinear optical medium via Maxwell's equations in nonlinear

dielectrics. In Bloembergen and Pershan (BP) theory, the boundary conditions at the interface of linear and nonlinear medium, harmonic intensity, polarization as well as linear and nonlinear Fresnel factors are clearly given. To verify BP theory, various second harmonic experiments in a variety of geometrical situations have been successfully carried out. In 1963 Ducuing and Bloembergen performed the first reflected SHG experiment investigating the optical laws of nonlinear second harmonic in reflection from GaAs crystal by using ruby laser light as an incident beam. Ducuing and Bloembergen (1963) confirmed the BP theory from the observation of dependence of intensity and polarization of the harmonic beam on crystallographic orientation. Moreover, the intensity of the reflected second harmonic light from GaAs was also measured as a function of the incident angle of Q-switched laser beam by Chang and Bloembergen (1965). In particular, the distinguishable nonlinear Brewster angle of reflected SHI was observed with the harmonic electric field in plane of incidence. However, in their experiment with GaAs, the pronounced dip of detectable SHI was not distinct due to the imaginary part of refractive index of the crystal. Later on, Lee and Bhanthumnavin (1976) successfully observed a very distinct nonlinear Brewster angle in KDP using ND: Glass as a fundamental beam. Bloembergen and Lee (1966) have demonstrated the maximum reflected SHI experiment from KDP crystal under the phase matching technique at total reflection. In 1969, Bloembergen, Simon, and Lee observed the direction, polarization and intensity of second harmonic light as a function of the incident angle in  $\text{NaClO}_3$  crystal and verified total reflection phenomena in SHG of light. In their experiment, three harmonic waves in reflection and transmission were studied with special emphasis on the region near the critical angle,  $\theta_w^{cr}$ , under the different crystal and polarization orientation. Bhanthumnavin

and Lee (1990) performed the experiment of reflected and transmitted SHG from KDP crystal and observed the null of SHI at normal incidence when the fundamental beam was Nd: Glass laser with the polarization perpendicular to the plane of incidence. By using an orientation of  $\vec{P}_{2w}^{NLS}$  of ADP crystal at the phase matching condition, Bhanthumnavin and Ampole (1990) not only demonstrated the maximum of reflected SHI at total reflection but also minimum of the reflected SHI at the nonlinear Brewster angle. Furthermore by using the KDP crystal, Bhanthumnavin and Lee (1994) experimentally observed the maximum reflected SHI at the phase matchable second harmonic generation at total reflection and also the minimum reflected SHI at the nonlinear Brewster angle of KDP crystal verifying their theoretical predictions. Suripon and Bhanthumnavin (1999) have theoretically shown the other pronounced dip of SHI at new nonlinear Brewster angle of ADP crystal.

This study investigates the reflected second harmonic generation at total reflection in the other wavelength of the fundamental beam. In this proposal a 900 nm ultrashort pulsed laser passing through the linear medium, 1-bromonaphthalene will be incident on the less-dense nonlinear medium, rubidium dihydrogen phosphate (RDP). The reflected second-harmonic intensity will be computed as a function of the incident angle. The nonlinear Brewster angle and phase matching condition will be investigated for minimum and maximum second-harmonic intensities. By using different crystallographic orientations of RDP crystal, a new nonlinear Brewster angle and variation of maximum SHI as a function of incident angles will be studied and compared to previous results of similar situations.

## 1.2 Research Objective

The main propose is to study reflected second-harmonic intensity ( $I_{2w}^R$ ) from  $\bar{4}2$  m-class crystal, especially, rubidium dihydrogen phosphate (RDP). The variation of  $I_{2w}^R$  will depend on the incident angle ( $\mathbf{q}_i$ ) and  $\vec{P}_{2w}^{NLS}$  orientation of the crystal. Also in this study, it is intended to study for new nonlinear Brewster angles ( $\mathbf{q}^{NB}$ ) occurring at different orientation of nonlinear polarization ( $\vec{P}_{2w}^{NLS}$ ).

## 1.3 Research Hypothesis

It is expected from this research that, the nonlinear Brewster Angle in RDP will occur at different  $\vec{P}_{2w}^{NLS}$  orientations. Furthermore it is anticipated that a phase matching condition for higher second harmonic intensity at total reflection will be achieved at the wavelength of 900 nm.

## 1.4 Scope and Limitations of the Study

In this study, the ultrafast laser pulses are utilized as incident pulses in order to create second-harmonic intensity,  $I_{2w}^R$ . The wavelength of the incident laser is at  $\lambda = 900$  nm with polarization being in  $[1\bar{1}0]$  direction with respect to the crystallographic axes of the RDP crystal. In order to facilitate a condition of total reflection, an

isotropic medium of higher index of refraction than of the RDP is required. In order to achieve this, 1-bromonaphthalene is employed as medium in which RDP is immersed. The direction of  $\vec{P}_{2w}^{NLS}$  is conducted to be in the optical axis of RDP crystal and also in the plane of incidence.

The C++ program and Microsoft Excel will be used for investigation the quantitative study of SHG in reflection with oblique incidence of the fundamental beam. The special emphasis is on the vicinity of the critical angle of the fundamental beam. Furthermore, the existence of the nonlinear Brewster angle will be theoretically demonstrated.

## CHAPTER II

### THEORY

Lasers can generate coherent radiation at many wavelengths utilized for various applications in nowadays. However, during the time that laser was under development, many wavelengths of coherent light were not available. The nonlinear optical effects in material are a major effort in order to generate frequencies that were not available and tunable as well. Therefore, other useful wavelengths involving second harmonic generation as first presented by Franken et al. (1962), were produced on the basics of the nonlinear interactions of the fundamental laser beam as the initiating source.

#### 2.1 Polarization in an Anisotropic Crystal

Nonlinear interactions between the fundamental laser beam, applied electric field  $\vec{E}$ , and nonlinear optical medium (anisotropic) crystal, can be demonstrated by the nonlinear response, induced nonlinear polarization  $\vec{P}^{NLS}$ . The response between the applied field and nonlinear polarization is described by means of a susceptibility tensor,  $\mathbf{C}$ , representing the material property of the crystal. In the case of second

harmonic generation, the tensor susceptibility can be shown to be of second order,  $\epsilon_{ij}$ . Thus second harmonic generation (SHG) can be radiated by the nonlinear polarization at twice frequency of the fundamental beam inside the anisotropic crystal with second-order nonlinear optical susceptibility.

### 2.1.1 Uniaxial Crystal and Its Index of Ellipsoid

There are two types of anisotropic crystal according to symmetry: uniaxial and biaxial crystals where each category is a function of symmetry. Crystals with trigonal, tetragonal and hexagonal symmetries are all uniaxial, whereas crystals with orthorhombic, monoclinic and triclinic symmetries are biaxial. For biaxial crystals, there is no orientation for which the index is the same for two orthogonal polarizations. Particularly, in a uniaxial crystal there exists one orientation of the crystal for which the index of refraction and wave velocity are independent of the polarization of the beam defined in the direction of the optic axis (z-axis) of the crystal. Thus there are two identical refractive indices while the other orthogonal direction has different refractive index. In this study, the negative uniaxial crystal, RDP, is a nonlinear crystal for SHG.

The refractive index of uniaxial crystal can be expressed in a form of index of ellipsoid as, (Hecht, 1987):

$$\frac{x^2 + y^2}{n_o^2} + \frac{z^2}{n_e^2} = 1 \quad (2.1)$$

where the  $n_o$  is the refractive index of wave polarization perpendicular to the optic axis, called ordinary, while  $n_e$  is refractive index of wave, called extraordinary. If  $n_e < n_o$ , crystal is called negative uniaxial, on the other hand, if it is positive uniaxial crystal then  $n_e > n_o$ , (Vendeyen, 1995) as shown in figure 2.1.

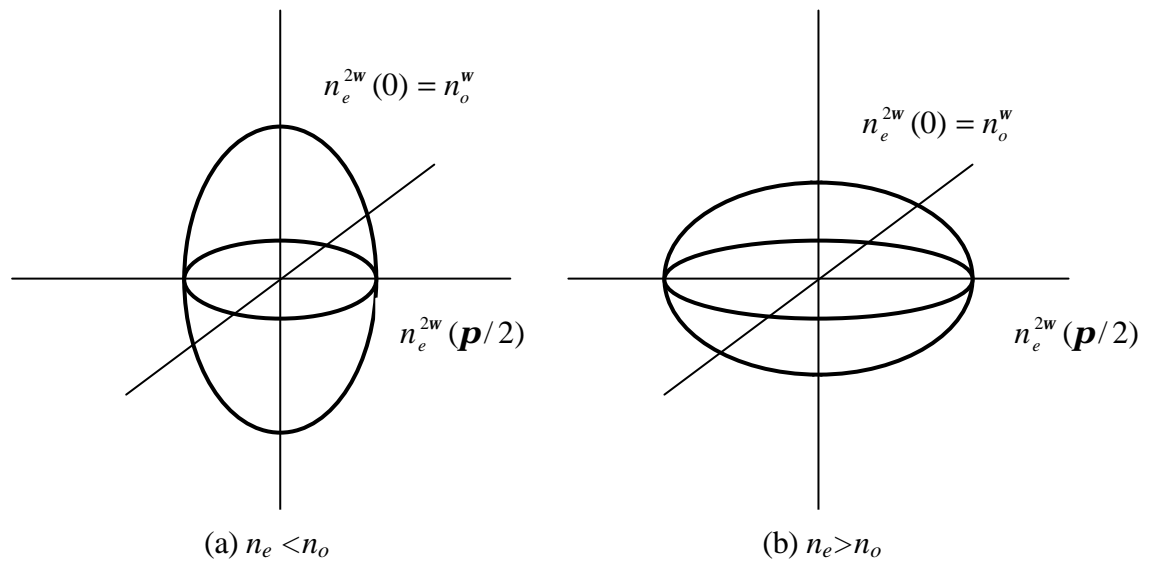


**Figure 2.1.** Refractive Index of (a) a negative (b) a positive uniaxial crystal

Because a uniaxial crystal has circular symmetry about the z (optic) axis, its optical properties depend only on the polar angle  $\mathbf{q}$  that the wave vector  $\vec{k}$  makes with the optic axis and not on the azimuthal orientation of  $\vec{k}$  relative to the x and y axis. Thereby, the index of ellipsoid, (Nye, 1976) can be defined as

$$\frac{1}{n_e^2(\mathbf{q})} = \frac{\cos^2 \mathbf{q}}{n_o^2} + \frac{\sin^2 \mathbf{q}}{n_e^2} \quad (2.2)$$

where  $\mathbf{q}$  is the angle between  $\vec{k}$  and z axis, as shown in figure 2.2.

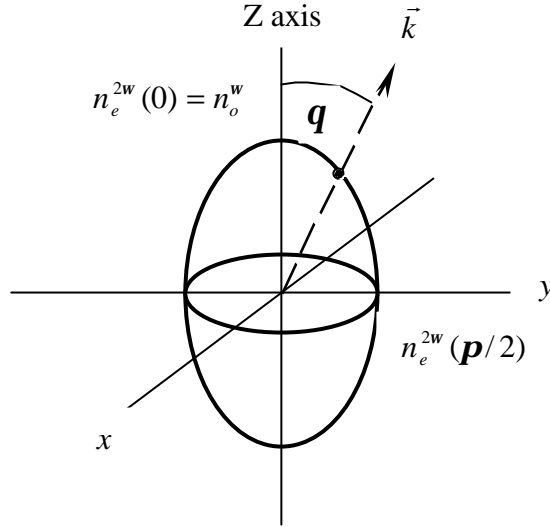


**Figure 2.2.** The intersection of  $\vec{k}$  and the surface of ellipsoid is indicated for  $n_e(\mathbf{q})$

### 2.1.2 Physical Origin of Polarization in Isotropic and Anisotropic Medium

Due to the response of the medium to the applied electric field, the induced polarization can be radiated inside the isotropic medium for the linear case expressed as

$$\vec{P} = \mathbf{e}_0 (\mathbf{c}_i^{(1)} \vec{E}) \quad (2.4)$$

For an anisotropic crystal with strong applied  $\vec{E}$ , the polarization  $\vec{P}$  can be expressed by a power series as follows,

$$\vec{P} = \mathbf{e}_0 (\mathbf{c}_i^{(1)} \vec{E} + \mathbf{c}_{ij}^{(2)} \vec{E}\vec{E} + \mathbf{c}_{ijk}^{(3)} \vec{E}\vec{E}\vec{E} + \dots) \quad (2.5)$$

Equation (2.4) is a combination of the linear and nonlinear polarization terms presented by  $\epsilon_o \mathbf{C}_i^{(1)} \vec{E}$  and  $\epsilon_o \mathbf{C}_{ij}^{(2)} \vec{E}\vec{E} + \epsilon_o \mathbf{C}_{ijk}^{(3)} \vec{E}\vec{E}\vec{E} + \dots$ , respectively. The induced optical polarization of the dielectric medium is due mostly to the loosely bound valence electrons that are displaced by the applied field and can be demonstrated as electron oscillation. Denoting the electron deviated from the equilibrium position by  $\vec{x}$  and the density of electron by  $N$ , the polarization  $\vec{P}$  is given by

$$\vec{P} = -Nex \quad (2.6)$$

### 2.1.2.1 Linear Polarization

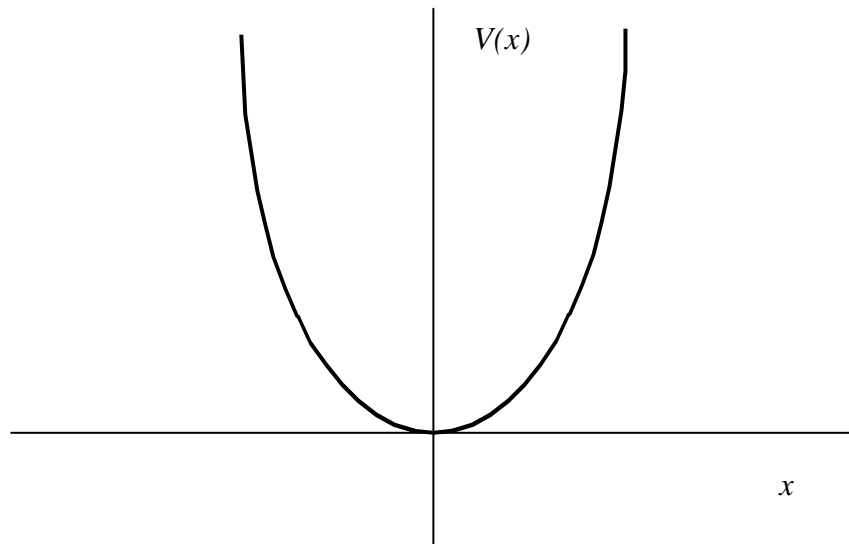


**Figure 2.3.** Symmetrical potential energy in linear medium

In a symmetric or isotropic crystal, the potential of an electron must reflect the crystal symmetry, so  $V(x) = V(-x)$  then symmetry  $V(x)$  contains only even powers of  $x$  by

$$V(x) = \frac{m}{2} \mathbf{w}_o^2 x^2 + \frac{m}{4} Bx^3 + \dots \quad (2.7)$$

where  $\mathbf{w}_o^2$  and  $B$  are constants and  $m$  is the electron mass. The restoring force on an electron is

$$\vec{F} = -\frac{\partial V}{\partial x} = -m\mathbf{w}_o^2 \bar{x} - mB\bar{x}^3 + \dots \quad (2.8)$$

and is zero at the equilibrium position  $x = 0$ .

Considered a low frequency electric field  $E(t)$  with Fourier components at small frequencies compared to  $\mathbf{w}_o$ . The excursion  $x$  caused by this field is found by equating the total force on the electron to zero.

$$-e\vec{E} - m\mathbf{w}_o^2 \bar{x} = 0$$

so that

$$\bar{x} = -\frac{e}{m\mathbf{w}_o^2} \vec{E}$$

This resulting in a induced polarization,  $\vec{P} = -Ne\vec{x}$ , whose is instantaneously proportional to the applied field or

$$\vec{P} \propto \vec{E} \quad (2.9)$$

That is defined as linear polarization,  $\vec{P}^L$ , which response to the applied electric field within a symmetric crystal is shown in figure 2.5 (a)

### 2.1.2.2 Nonlinear Polarization

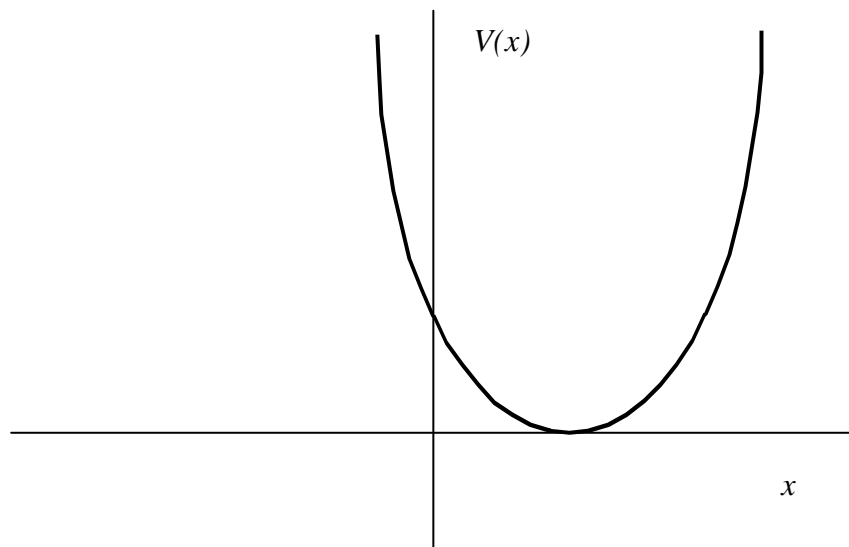


**Figure 2.4.** Asymmetrical potential energy in nonlinear medium

In an asymmetric or anisotropic medium (noncentrosymmetric type) in which the condition  $V(x) \neq V(-x)$ , the potential function can contain odd powers of  $x$  and thus

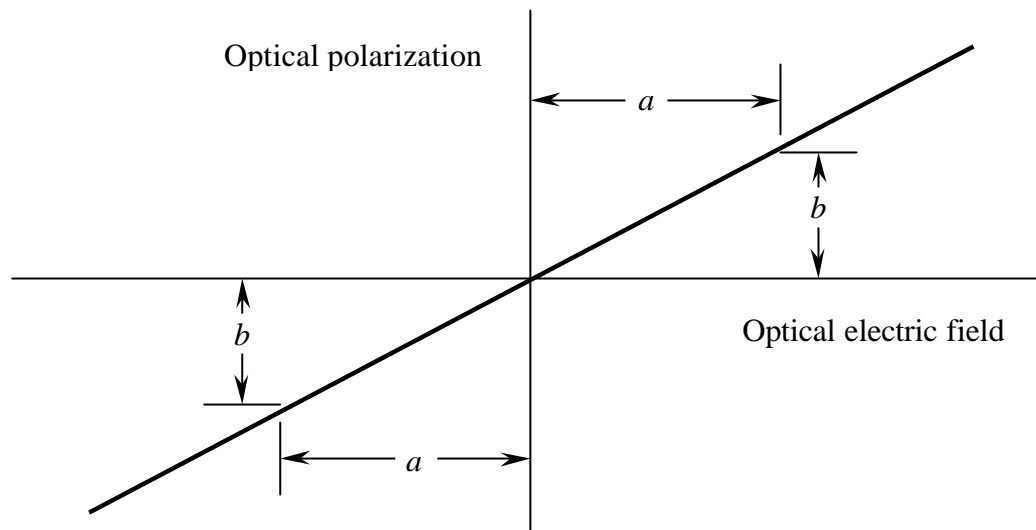
$$V(x) = \frac{m\mathbf{w}_o^2}{2}x^2 + \frac{m}{3}Dx^3 + \dots \quad (2.10)$$

corresponding to a restoring force on the electron

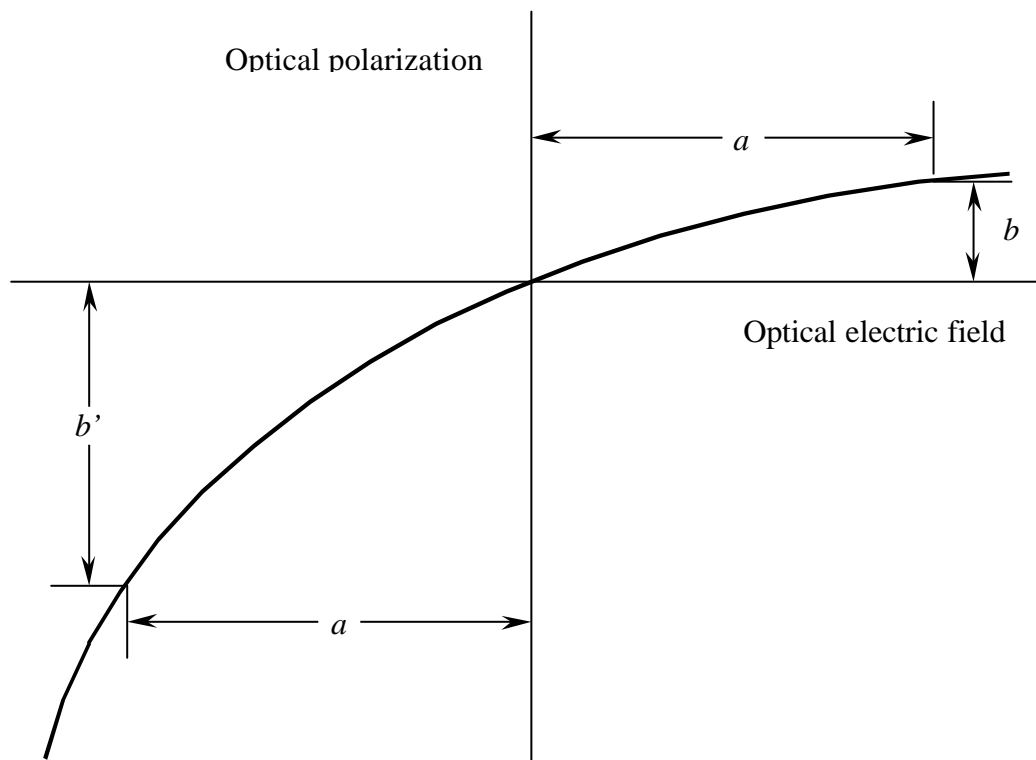
$$\vec{F} = -\frac{\partial V}{\partial x} = -m\mathbf{w}_o^2\vec{x} - mD\vec{x}^2 + \dots \quad (2.11)$$

If  $D > 0$ , it follows immediately that if the electric force on the electron is positive ( $\vec{E} < 0$ ), the induced polarization is smaller than when the field direction is reversed as shown by figure 2.5 (b).

For an alternating electric field at  $\mathbf{w}$  applied to the crystal, if the crystal is linear, the induced polarization oscillates at  $\mathbf{w}$  as shown in figure 2.6 (a). But in a nonlinear crystal the induced nonlinear polarization in the positive peak (b) is smaller than the negative one ( $b'$ ) due to the stiffer restoring force at  $x > 0$  as in figure 2.6 (b). Using a Fourier series to analysis the nonlinear polarization wave, the average (dc) term, the fundamental and second harmonic components are plotted in figure 2.7.



(a)



(b)

**Figure 2.5.** Relation between induced polarization and the electric field causing it (a) in a symmetric and (b) asymmetric crystal.

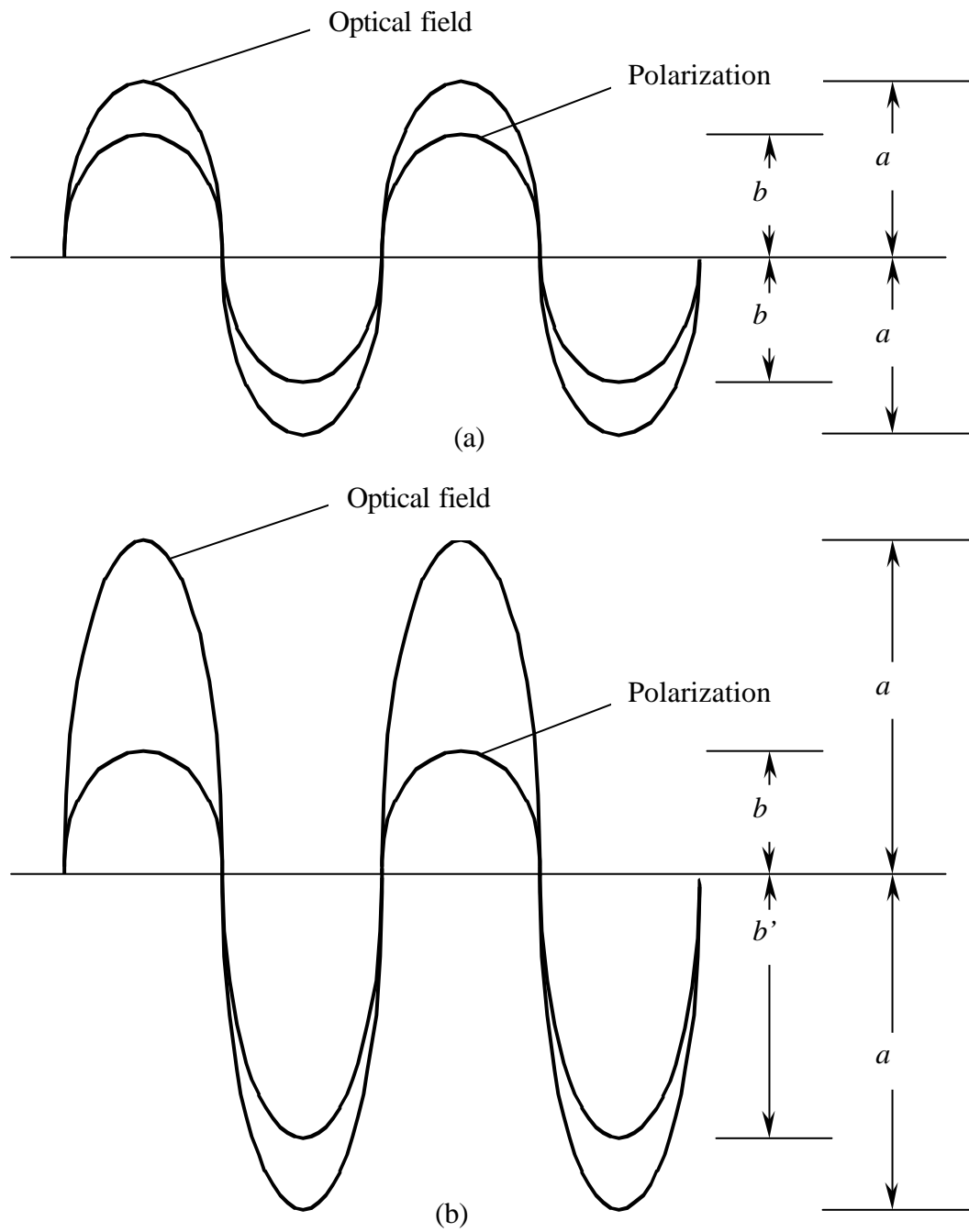


**Figure 2.6.** An applied sinusoid electric field and the resulting polarization in (a) symmetric and (b) asymmetric crystal

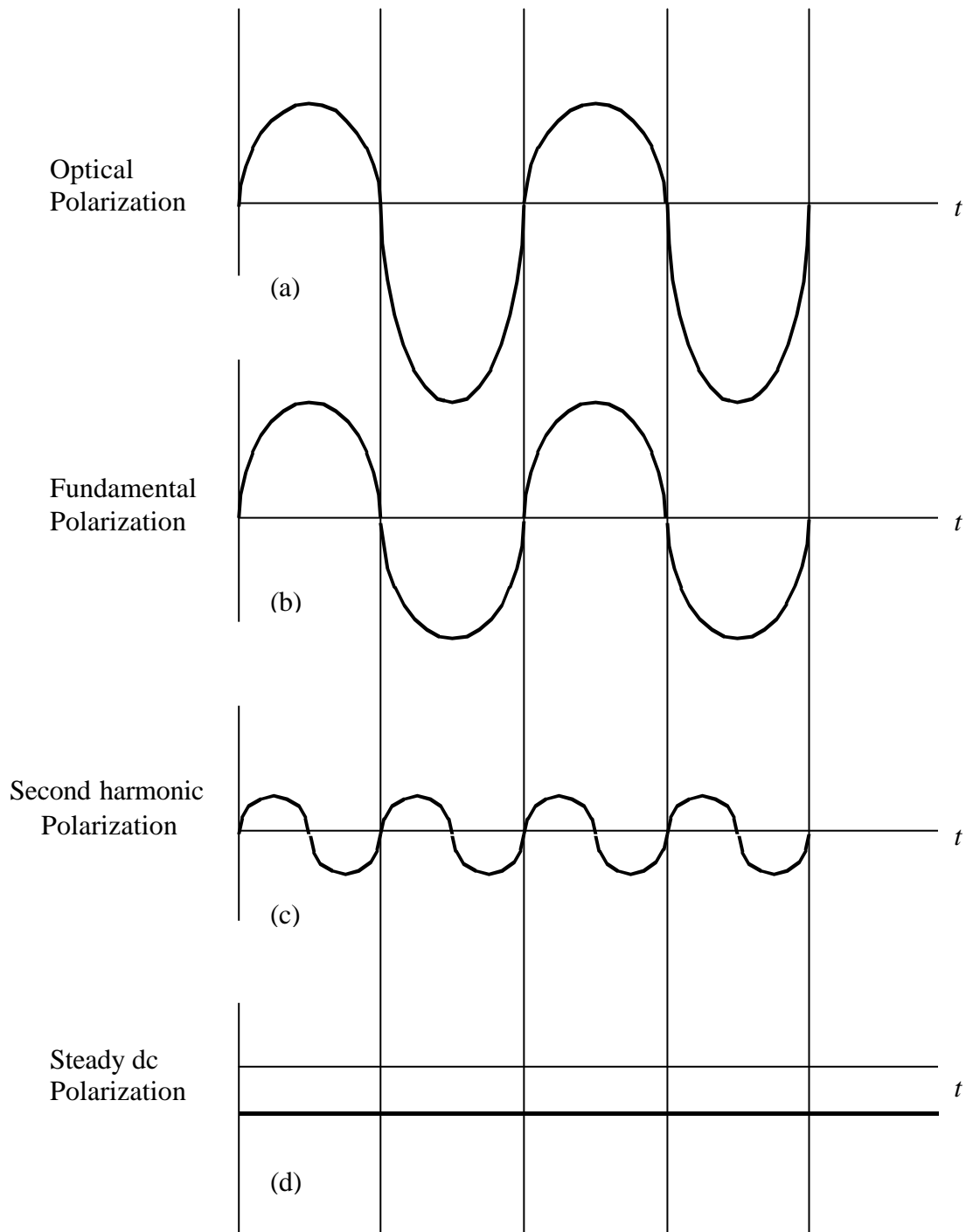


**Figure 2.7.** Analysis of the nonlinear polarization wave (a) of figure 2.6 (b) shown that it contains components oscillation at (b) the same frequency ( $\omega$ ) as the wave inducing it, (c) twice that frequency ( $2\omega$ ) and (d) an average (dc) negative component.

To relate the nonlinear polarization formally to the inducing field, we use equation for the restoring force and take the driving electric field as  $E^w \cos \mathbf{w} t$  by

$$\frac{d^2}{dt^2} x(t) + \mathbf{S} \frac{d}{dt} x(t) + \mathbf{w}_0^2 x(t) + D x^2(t) = -\frac{e E^w}{2m} (e^{i\mathbf{w}t} + e^{-i\mathbf{w}t}). \quad (2.12)$$

Then the nonlinear polarization at  $2\mathbf{w}$  is

$$\vec{P}_{2\mathbf{w}}^{NLS}(t) = \mathbf{C}^{2\mathbf{w}} [E^w]^2 \cdot e^{2i\mathbf{w}t} + c.c.$$

where c.c. is the complex components of  $\vec{P}_{2\mathbf{w}}^{NLS}(t)$ .

Given  $\vec{P}_{2\mathbf{w}}^{NLS}(t)$ , the complex amplitude of the polarization, we have

$$\vec{P}_{2\mathbf{w}}^{NLS}(t) = P_{2\mathbf{w}}^{NLS} \cdot e^{i2\mathbf{w}t} + c.c.,$$

or

$$P_i^{NLS}(2\mathbf{w}) = \sum_{j,k=x,y,z} \mathbf{C}_{ijk}^{2\mathbf{w}} E^j E^k. \quad (2.13)$$

Equation (2.13) is a scalar equation. Thus the induced nonlinear polarization,  $\vec{P}_{2\mathbf{w}}^{NLS}$  can be written in matrix form using the second order susceptibility,  $\mathbf{C}_{ij}$ .

$$\begin{pmatrix} P_x \\ P_y \\ P_z \end{pmatrix}_{2\mathbf{w}}^{NLS} = \mathbf{e}_o \begin{pmatrix} \mathbf{c}_{11} & \mathbf{c}_{12} & \mathbf{c}_{13} & \mathbf{c}_{14} & \mathbf{c}_{15} & \mathbf{c}_{16} \\ \mathbf{c}_{21} & \mathbf{c}_{22} & \mathbf{c}_{23} & \mathbf{c}_{24} & \mathbf{c}_{25} & \mathbf{c}_{26} \\ \mathbf{c}_{31} & \mathbf{c}_{32} & \mathbf{c}_{33} & \mathbf{c}_{34} & \mathbf{c}_{35} & \mathbf{c}_{36} \end{pmatrix} \begin{pmatrix} E_x^2 \\ E_y^2 \\ E_z^2 \\ E_z E_x \\ E_y E_z \\ E_x E_y \end{pmatrix}_{\mathbf{w}} \quad (2.14)$$

In crystal processing with inversion symmetry, all the nonlinear coefficients  $\mathbf{c}_{ijk}$  must be zero. This follows directly from the equation (2.14). By reversing the direction of the electric field,  $E_j^w$  becomes  $-E_j^w$  and  $E_k^w$  becomes  $-E_k^w$ . Since the crystal is centrosymmetric, the new induced polarization,  $P_{2\mathbf{w}}^L$ , produced by the reversed electric field must be the same relationship to the original electric field, that is

$$-P_i^L(2\mathbf{w}) = \sum_{jk} \mathbf{c}_{ijk}^{2w} (-E_j^w)(E_k^w). \quad (2.15)$$

Equation (2.15) can hold simultaneously only if  $\mathbf{c}_{ijk}^{2w}$  are all zero inferring no second harmonic generation in symmetric crystal.

## 2.2 Second Harmonic Generation in Reflection

The generation of waves at new frequencies in an anisotropic medium due to the nonlinear interaction will be investigated in the macroscopic by using Maxwell's equations since there is enough power density in a light beam from a coherent source. The solution of Maxwell's equations shows the behavior of light wave at the boundary of nonlinear media and describes how harmonic waves in both reflection and transmission commence to grow when a fundamental wave enters a nonlinear crystal. Especially useful is its description of second harmonic generation (SHG) phenomenon by nonlinear polarization,  $\vec{P}_{2\omega}^{NLS}$ . Besides the generation of the direction of light harmonic waves, Snell's law is extended as well as observation of second harmonic intensity (SHI).

### 2.2.1 Second Harmonic Waves Emanating from a Boundary

When a monochromatic plane wave at frequency  $\omega$  with perpendicular polarization to the plane of incidence passes through a uniaxial crystal, such as RDP crystal, the resulting second harmonic waves can be treated by Maxwell's equation for nonlinear medium as follows.

$$\begin{aligned}
 \nabla \times \nabla \times \vec{E} &= -\frac{1}{c} \frac{\partial}{\partial t} \mathbf{m}\vec{H}, \\
 \nabla \times \nabla \times \vec{H} &= \frac{1}{c} \frac{\partial}{\partial t} \vec{D} + \frac{4\mathbf{p}}{c} \vec{J}, \\
 \nabla \cdot \vec{D} &= 4\mathbf{p}\mathbf{r}; \text{ and} \\
 \nabla \cdot \vec{B} &= 0,
 \end{aligned} \tag{2.16}$$

with auxiliary equation

$$\vec{D} = \mathbf{e}_o \vec{E} + \vec{P} \quad (2.17)$$

For the nonlinear case, the polarization can be expressed as

$$\vec{P} = \vec{P}^L + 4\mathbf{p}\vec{P}^{NLS} = \mathbf{e}_o \mathbf{c}_L \vec{E} + 4\mathbf{p}\vec{P}^{NLS}. \quad (2.18)$$

Given  $\mathbf{e} = \mathbf{e}_o (1 + \mathbf{c}_L)$ , then

$$\vec{D} = \mathbf{e}\vec{E} + 4\mathbf{p}\vec{P}^{NLS}, \quad (2.19)$$

where  $\vec{E}$  is the electric field and  $\vec{H}$  is the magnetic field. Also  $\mathbf{m}$  and  $\mathbf{e}$  are the permeability and permittivity of the medium in which the wave propagates and  $c$  is the velocity of propagation in vacuum. For lossless, nonconducting and nonmagnetic medium,  $\mathbf{e}$  will be taken as a scalar and  $\mathbf{m}=1$ . The wave equation of the second harmonic is expressed as

$$\nabla \times \nabla \times \vec{E} + \frac{\mathbf{e}(2\mathbf{w})}{c} \frac{\partial^2}{\partial t^2} \vec{E} = -\frac{4\mathbf{p}}{c^2} \frac{\partial^2}{\partial t^2} \vec{P}_{2w}^{NLS}, \quad (2.20)$$

or

$$\nabla^2 \vec{E} - \frac{\mathbf{e}(2\mathbf{w})}{c^2} \frac{\partial^2}{\partial t^2} \vec{E} = \frac{4\mathbf{p}}{c^2} \frac{\partial^2}{\partial t^2} \vec{P}_{2w}^{NLS}. \quad (2.21)$$

Solution of (2.21) comprises the homogeneous and inhomogeneous solutions, due to the driving term,  $\vec{P}_{2w}^{NLS}$ , on the right hand side. The  $\vec{P}_{2w}^{NLS}$  arising from the

nonlinear susceptibility,  $\mathbf{C}_{ij}^{NL}$ , will radiate energy at second harmonic frequencies,  $2\boldsymbol{\omega}$ , and can be shown by

$$\hat{p}P^{NLS} = \vec{P}_{2\boldsymbol{\omega}}^{NLS} = \boldsymbol{\alpha}(2\boldsymbol{\omega})\vec{E}_w^T\vec{E}_w^T \exp i(\vec{k}^S \cdot \vec{r} - 2\boldsymbol{\omega}t). \quad (2.22)$$

In RDP crystal, the solutions of inhomogeneous wave equation are

$$\begin{aligned} \vec{E}_{2\boldsymbol{\omega}}^T &= \hat{e}^T E_{2\boldsymbol{\omega}}^T \exp i(\vec{k}_{2\boldsymbol{\omega}}^T \cdot \vec{r} - 2\boldsymbol{\omega}t) - \frac{4\vec{P}_{2\boldsymbol{\omega}}^{NLS} (4\boldsymbol{\omega}^2 / c^2)}{(\vec{k}_{2\boldsymbol{\omega}}^T)^2 - (\vec{k}_{2\boldsymbol{\omega}}^S)^2} \\ &\quad \times \left[ \hat{p} - \frac{\vec{k}_{2\boldsymbol{\omega}}^S (\vec{k}_{2\boldsymbol{\omega}}^S \cdot \hat{p})}{(\vec{k}_{2\boldsymbol{\omega}}^T)^2} \right] \exp i(\vec{k}_{2\boldsymbol{\omega}}^S \cdot \vec{r} - 2\boldsymbol{\omega}t), \text{ and} \\ \vec{H}_{2\boldsymbol{\omega}}^T &= \frac{c}{2\boldsymbol{\omega}} (\vec{k}_{2\boldsymbol{\omega}}^T \times \hat{e}^T) E_{2\boldsymbol{\omega}}^T \exp i(\vec{k}_{2\boldsymbol{\omega}}^T \cdot \vec{r} - 2\boldsymbol{\omega}t) \\ &\quad - \frac{4\vec{P}_{2\boldsymbol{\omega}}^{NLS} (4\boldsymbol{\omega}^2 / c^2)}{(\vec{k}_{2\boldsymbol{\omega}}^T)^2 - (\vec{k}_{2\boldsymbol{\omega}}^S)^2} \frac{c}{2\boldsymbol{\omega}} (\vec{k}_{2\boldsymbol{\omega}}^S \times \hat{p}) \exp i(\vec{k}_{2\boldsymbol{\omega}}^S \cdot \vec{r} - 2\boldsymbol{\omega}t). \end{aligned} \quad (2.23)$$

In vacuum the solutions of homogeneous wave equation are,

$$\begin{aligned} \vec{E}_{2\boldsymbol{\omega}}^R &= \hat{e}^R E_{2\boldsymbol{\omega}}^R \exp i(\vec{k}_{2\boldsymbol{\omega}}^R \cdot \vec{r} - 2\boldsymbol{\omega}t), \text{ and,} \\ \vec{H}_{2\boldsymbol{\omega}}^R &= \frac{c}{2\boldsymbol{\omega}} (\vec{k}_{2\boldsymbol{\omega}}^R \times \hat{e}^R) E_{2\boldsymbol{\omega}}^R \exp i(\vec{k}_{2\boldsymbol{\omega}}^R \cdot \vec{r} - 2\boldsymbol{\omega}t). \end{aligned} \quad (2.24)$$

The geometry of incident, reflected and transmitted waves are sketched in figure 2.8. For the wave vector of the fundamental wave,  $\vec{k}_w^i$ , with polarization perpendicular to the plane of incidence passing from a linear through a nonlinear medium, the  $\vec{P}_{2\boldsymbol{\omega}}^{NLS}$  will arise along the plane of incidence as well as with the

reflected and transmitted with wave vectors,  $\vec{k}_w^r$ ,  $\vec{k}_w^t$ ,  $\vec{k}_{2w}^R$ ,  $\vec{k}_{2w}^S$  and  $\vec{k}_{2w}^T$ . From figure 2.8, the directions of each wave vectors are identified with the angles made with the normal surface and will be used to derive for further information concerning the general laws of reflection and refraction.

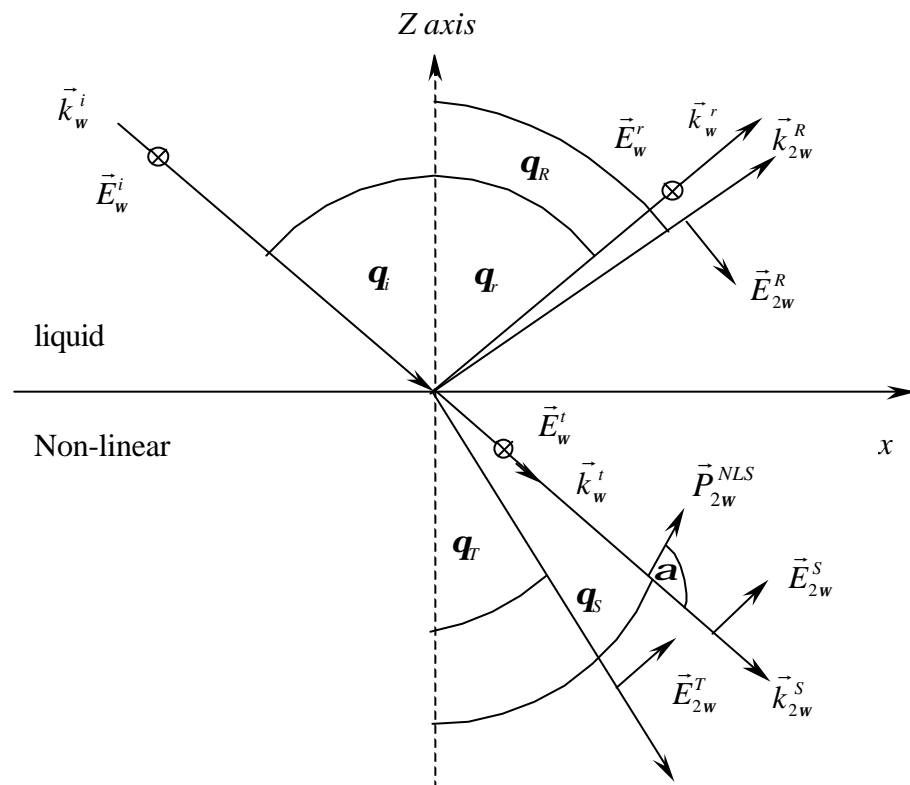


**Figure 2.8.** The incident, reflected, and transmitted rays at the fundamental and second harmonic frequencies near the boundary between a RDP crystal and linear medium.

### 2.2.2. Generalized Snell's Law

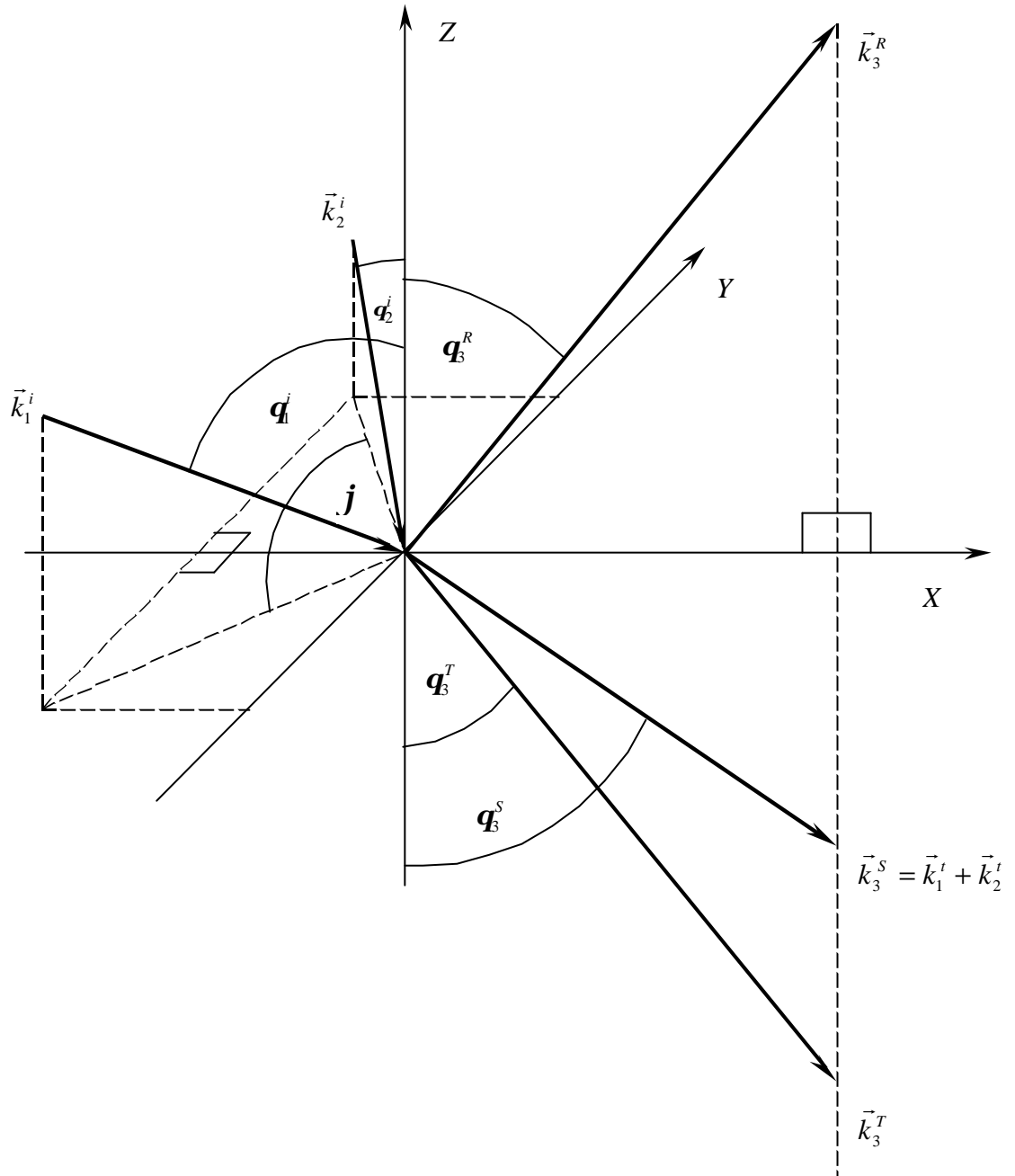


**Figure 2.9.** Two incident rays at frequencies  $\omega_1$  and  $\omega_2$  create a reflected wave, a homogeneous transmitted wave at the sum frequency  $\omega_3 = \omega_1 + \omega_2$ , all emanating from the boundary between the linear and nonlinear medium.

Consider a boundary ( $z=0$ ) between the linear and nonlinear medium. Two incident plane waves,  $\vec{E}_1 \exp i(\vec{k}_1^i \cdot \vec{r} - \mathbf{w}_1 t)$  and  $\vec{E}_2 \exp i(k_2^i \cdot \vec{r} - \mathbf{w}_2 t)$  simultaneously emanate reflected and transmitted waves at both frequencies  $\mathbf{w}$  and  $2\mathbf{w}$ . The geometry is defined in Fig 2.9. The angle of incidences of the two waves are  $\mathbf{q}_i^1$  and  $\mathbf{q}_i^2$ , the incident planes make an angle  $\mathbf{f}$  with each other. Choose the x and y directions of the coordinate system such that  $\vec{k}_{1y}^i = -\vec{k}_{2y}^i$ . This leads to the momentum conservation as for the sum wave.

$$\begin{aligned} k_{3x}^R &= k_{3x}^T = k_{3x}^S = k_{1x}^T + k_{2x}^T = k_{1x}^i + k_{2x}^i, \\ k_{3x}^R &= k_{3x}^T = k_{3y}^S = k_{1y}^T + k_{2y}^T = k_{1y}^i + k_{2y}^i = 0. \end{aligned} \quad (2.25)$$

From (2.25), the inhomogeneous source wave ( $\vec{k}_{2w}^S$ ); the homogeneous transmitted,  $\vec{k}_{2w}^T$ , and reflected waves at sum frequency lie in the same phase  $xz$  plane as well as the boundary normal and crystal optic axis.

The direction of inhomogeneous wave is given by  $\exp i\{(\vec{k}_1^T + \vec{k}_2^T) \cdot \vec{r} - i(\mathbf{w}_1 + \mathbf{w}_2)t\}$  and its angle with the normal  $\mathbf{q}_3^S$  is determined by

$$\sin \mathbf{q}_3^S = \left| \vec{k}_{1x}^T + \vec{k}_{2x}^T \right| / \left| \vec{k}_{1x}^T + \vec{k}_{2x}^T \right|. \quad (2.26)$$

Then (2.25) can be written by using (2.26) and simple trigonometry as shown

$$\begin{aligned}
|\vec{k}_3^T|^2 \sin^2 \mathbf{q}_3^T &= |\vec{k}_3^R|^2 \sin^2 \mathbf{q}_3^R \\
&= |\vec{k}_1^i|^2 \sin^2 \mathbf{q}_1^i + |\vec{k}_2^i|^2 \sin^2 \mathbf{q}_2^i \\
&= + 2|\vec{k}_1^i||\vec{k}_2^i| \sin \mathbf{q}_1^i \sin \mathbf{q}_2^i \cos \mathbf{f},
\end{aligned} \tag{2.27}$$

where all angles with the normal are defined in the interval 0 to  $\pi/2$ . The angle between the planes of incidence goes from 0 to  $\pi$ . Furthermore, (2.27) can also be written as

$$\begin{aligned}
\mathbf{e}_3^T \mathbf{w}_3^2 \sin^2 \mathbf{q}_3^T &= \mathbf{e}_3^R \mathbf{w}_3^2 \sin^2 \mathbf{q}_3^R \\
&= \mathbf{e}_1^R \mathbf{w}_1^2 \sin^2 \mathbf{q}_1^i + \mathbf{e}_2^R \mathbf{w}_2^2 \sin^2 \mathbf{q}_2^i + 2(\mathbf{e}_1^R \mathbf{e}_2^R)^{1/2} \mathbf{w}_1 \mathbf{w}_2 \sin \mathbf{q}_1^i \sin \mathbf{q}_2^i \cos \mathbf{f},
\end{aligned} \tag{2.28}$$

since  $\mathbf{e} = k^2 \left( \frac{\mathbf{w}^2}{c^2} \right)^{-1}$ . Then, an effective dielectric constant  $\mathbf{e}^S$  for nonlinear source

wave can be defined by

$$\mathbf{e}_3^S \sin^2 \mathbf{q}_3^S = \mathbf{e}_3^T \sin^2 \mathbf{q}_3^T = \mathbf{e}_3^R \sin^2 \mathbf{q}_3^R \tag{2.29}$$

In this study, the planes of incidence coincide on the same side, and  $\mathbf{w}_3 = 2\mathbf{w}$  since  $\mathbf{w}_1 = \mathbf{w}_2$ , Then  $\mathbf{e}_1^R = \mathbf{e}_2^R$ ,  $\mathbf{f} = 0$  and  $\mathbf{q}_1^i = \mathbf{q}_2^i$ . A simple relationship can be introduced:

$$(\mathbf{e}_3^T)^{1/2} \sin \mathbf{q}_3^T = \frac{\mathbf{w}_1}{\mathbf{w}_2} (\mathbf{e}_1^R)^{1/2} \sin \mathbf{q}_1^i + \frac{\mathbf{w}_2}{\mathbf{w}_3} (\mathbf{e}_2^R)^{1/2} \sin \mathbf{q}_2^i,$$

or

$$\left(\mathbf{e}_3^T\right)^{1/2} \sin \mathbf{q}_B^T = \left(\mathbf{e}_1^R\right)^{1/2} \mathbf{q}^i,$$

or

$$\sqrt{\mathbf{e}_1^i} \sin \mathbf{q}_1^i = \sqrt{\mathbf{e}_3^T} \sin \mathbf{q}_B^T = \sqrt{\mathbf{e}_3^S} \sin \mathbf{q}_S^S, \quad (2.30)$$

when refractive index  $n = \sqrt{\mathbf{e}}$ . Thus

$$n_w^L \sin \mathbf{q}_i = n_{2w}^{NL} \sin \mathbf{q}_T = n_{2w}^{NL} \sin \mathbf{q}_R = n_w^{NL} \sin \mathbf{q}_S, \quad (2.31)$$

where  $n_w^L$  the refractive indices of the linear medium at  $\omega$  which  $n_w^{NL}$ ,  $n_{2w}^{NL}$  are the refractive index of nonlinear medium of  $2\mathbf{w}$  respectively.

### 2.2.3 Polarization in Plane of Incidence and Second Harmonic Intensity in Reflection

Second harmonic generation can occur by nonlinear polarization,  $\vec{P}_{2w}^{NLS}$ , identified as the inhomogeneous part of Maxwell's equation. The induced nonlinear polarization at frequency  $\mathbf{w}_3 = \mathbf{w}_1 + \mathbf{w}_2$ , by the two incident waves of  $\mathbf{w}_1 + \mathbf{w}_2 = 2\mathbf{w}$  can be presented by

$$\vec{P}_{2w}^{NLS} = \mathbf{C}_{2w}^{NLS} \vec{E}_w^T \vec{E}_w^T \exp i \left[ (\vec{k}_1^t + \vec{k}_2^t) \cdot \vec{r} - 2\mathbf{w}t \right], \quad (2.32)$$

and  $\vec{k}_3^S = \vec{k}_1^t + \vec{k}_2^t$ .

From (2.32) both magnitude and direction of  $\vec{P}_{2w}^{NLS}$  depend on the nonlinear susceptibility,  $\mathbf{C}_{2w}^{NL}$ , and the transmitted wave at fundamental frequency  $\vec{E}_w^T$ , given in the formulas of Snell and Fresnel for the incident beam.

The decomposition of  $\vec{P}_{2w}^{NLS}$ , along and normal to plane of incidence, might account for its directional dependence, since in the preceding section,  $\vec{P}_{2w, //}^{NLS}$  and  $\vec{P}_{2w, \perp}^{NLS}$  are independent from each other. Furthermore, the angular dependence  $\vec{P}_{2w}^{NLS}$  can be divided from transmitted wave through a function of the fundamental wave  $\vec{E}_w^T$  by the usual Fresnel equation. Therefore, the nonlinear polarization along the plane of incidence;  $\vec{P}_{2w, //}^{NLS}$  inside the RDP crystal can be treated by the incident vector perpendicular to that one,  $\vec{E}_{w, \perp}^i$  or  $\vec{E}_y^i = \vec{P}_y^{NLS} = 0$ .

The nonlinear polarization in the plane of incidence by its magnitude  $P_{2w}^{NLS}$  makes an angle  $\mathbf{a}$  with the direction of propagation of generating source  $\vec{k}_{2w}^S$ . The second harmonic wave is shown in figure 2.10. The SHG can be investigated from (2.23) and (2.24) by the continuity of the tangential components at  $z = 0$ .

$$E_x = -E_{//}^R \cos \mathbf{q}_R = E_{//}^T \cos \mathbf{q}_T + \frac{4\mathbf{p}_{//}^{NLS} \sin \mathbf{a} \cos \mathbf{q}_S}{\mathbf{e}_S - \mathbf{e}_T} - \frac{4\mathbf{p}_{//}^{NLS} \cos \mathbf{a} \sin \mathbf{q}_S}{\mathbf{e}_T}, \text{ and, (2.33)}$$

$$H_y = -\mathbf{e}_R^{1/2} E^R = -\mathbf{e}_T^{1/2} \mathbf{e}_{11}^T - \mathbf{e}_S^{1/2} \frac{4\mathbf{p}_{//}^{NLS} \sin \mathbf{a}}{\mathbf{e}_S - \mathbf{e}_T}. \quad (2.34)$$

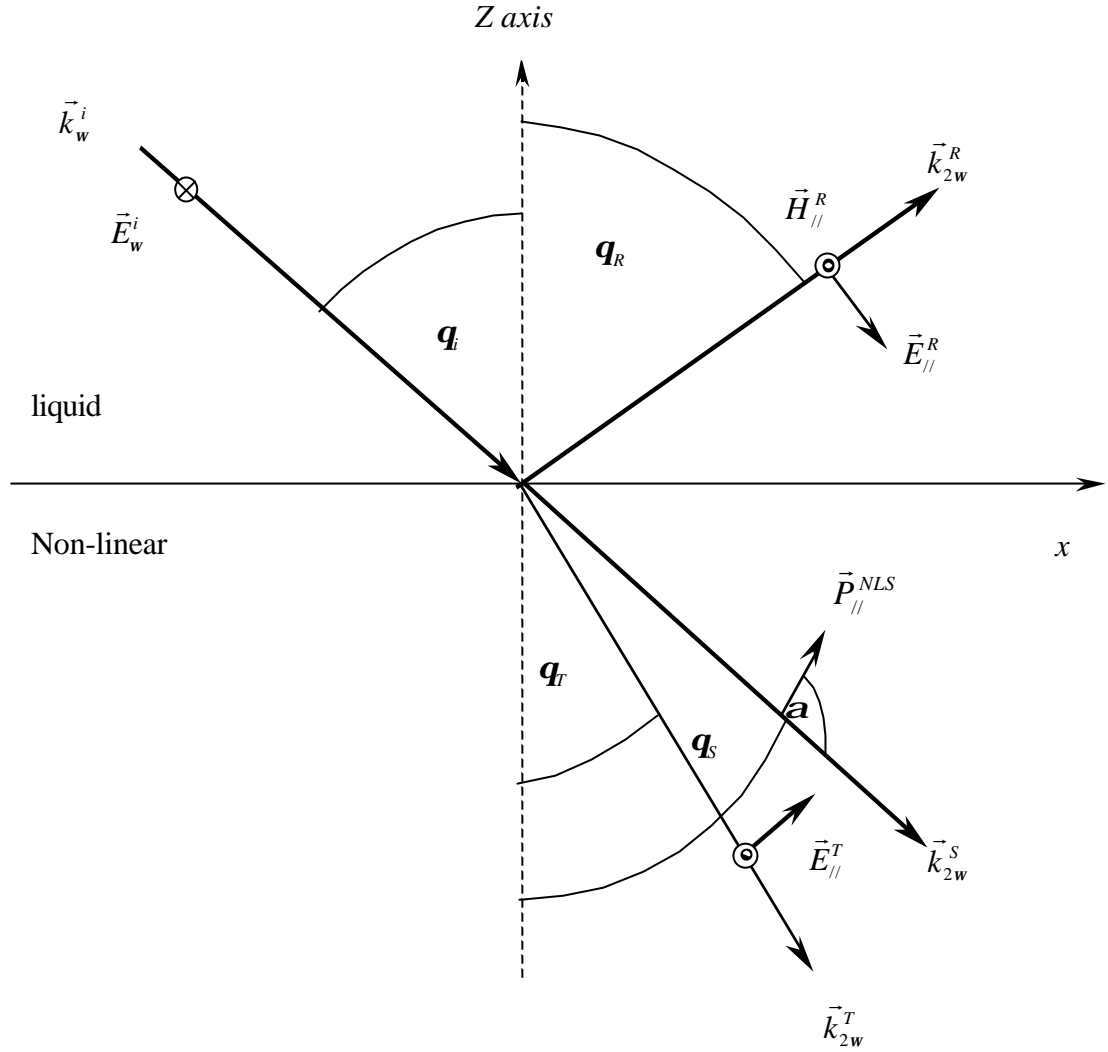


**Figure 2.10.** The harmonic wave at the boundary of a nonlinear medium, with electric field vector in the plane of reflection, the nonlinear polarization and lies in the plane of incidence.

By substitution of  $E_{//}^T$  of (2.34) into (2.33), the amplitude of the reflected electric field at second harmonic frequencies is given by

$$E_{//}^R = \frac{4\mathbf{p}_{//}^{NLS} \sin a}{\sqrt{\mathbf{e}_R} \cos \mathbf{q}_T - \sqrt{\mathbf{e}_T} \cos \mathbf{q}_R} \left[ \frac{1 - (\mathbf{e}_S - \mathbf{e}_T)^{-1} \mathbf{e}_R \sin \mathbf{q}_R}{\sqrt{\mathbf{e}_S} \cos \mathbf{q}_i + \sqrt{\mathbf{e}_T} \cos \mathbf{q}_S} \right].$$

$$+ \frac{4\mathbf{p}_{//}^{NLS} \sin \mathbf{a}}{\sqrt{\mathbf{e}_R \mathbf{e}_R \mathbf{w} \cos \mathbf{q}_T - \mathbf{e}_T \cos \mathbf{q}_R}}. \quad (2.35)$$

This expression can be transformed by shell's equation in (2.28). Then  $E_{//}^R$  is given as

$$E_{//}^R = \frac{4\mathbf{p}_{//}^{NLS} \sin \mathbf{q}_S \sin^2 \mathbf{q}_T \sin(\mathbf{a} + \mathbf{q}_T + \mathbf{q}_S)}{\mathbf{e}_R \sin \mathbf{q}_R \sin(\mathbf{q}_T + \mathbf{q}_S) \sin(\mathbf{q}_T + \mathbf{q}_R) \cos(\mathbf{q}_T + \mathbf{q}_R)}. \quad (2.36)$$

$E_{//}^T$  simultaneously be derived by substituting  $E_{//}^R$  into (13) as

$$E_{//}^T = \sqrt{\frac{\mathbf{e}_R}{\mathbf{e}_T}} E_{//}^R - \sqrt{\frac{\mathbf{e}_S}{\mathbf{e}_T} \frac{4\mathbf{p}_{//}^{NLS} \sin \mathbf{a}}{(\mathbf{e}_S - \mathbf{e}_T)}}. \quad (2.37)$$

The significant component of  $E_{//}^R$  and  $E_{//}^T$  can be apparently seen by  $P_{//}^{NLS}$  term as the source of second harmonic wave at frequency  $2\mathbf{w}$ . Using the usual Fresnel equation,  $E_{//}^R$  can be written as

$$E_{//}^R(2\mathbf{w}) = 4\mathbf{p}_{//}^{NLS}(2\mathbf{w}) F_{R, //}^{NL}, \quad (2.38)$$

where  $F_{R, //}^{NL}$  is the nonlinear Fresnel factor in reflection when  $P_{2\mathbf{w}}^{NLS}$  lies the plane of incidence and have been calculated by BP theory. Comparing (2.38) with (2.36),

$F_{R, //}^{NL}$  is determined as:

$$F_{R, //}^{NL} = \frac{\sin \mathbf{q}_S \sin^2 \mathbf{q}_T \sin(\mathbf{a} + \mathbf{q}_S + \mathbf{q}_T)}{\mathbf{e}_R \sin \mathbf{q}_R \sin(\mathbf{q}_T + \mathbf{q}_S) \sin(\mathbf{q}_T + \mathbf{q}_R) \cos(\mathbf{q}_T + \mathbf{q}_R)}, \quad (2.39)$$

According to Bloembergen and Pershan (1962). The time-averaged second-harmonic power carried by the harmonic beam or second harmonic intensity is given by

$$I_{2w}^R = \mathbf{a} \frac{c}{8p} \sqrt{\mathbf{e}_R} |E_{2w}^R|^2 A_R, \quad (2.40)$$

where  $A_R$  is a cross-sectional area of the reflected wave and be calculated from (2.40)

$$A_R = (dd' \cos \mathbf{q}_R) / \cos \mathbf{q}_i. \quad (2.41)$$

In (2.41)  $dd'$  is the rectangular slit which defines the size of the incident laser beam.  $\mathbf{q}_R$  is the incident face normal;  $\mathbf{q}_i$  and  $\mathbf{q}_R$  are the incident and the reflected respectively.

Inside a  $\bar{4}2m$  uniaxial crystal such as KDP, ADP and RDP, the nonlinear susceptibility terms are reduced to  $\mathbf{c}_{14}$ ,  $\mathbf{c}_{25}$  and  $\mathbf{c}_{36}$ . Thus the relationship between  $P_{2w}^{NLS}$  and applied field at fundamental frequency is shown.

$$\begin{pmatrix} \vec{P}_x^{NLS}(2\mathbf{w}) \\ \vec{P}_y^{NLS}(2\mathbf{w}) \\ \vec{P}_z^{NLS}(2\mathbf{w}) \end{pmatrix} = \begin{pmatrix} 0 & 0 & 0 & \mathbf{c}_{14} & 0 & 0 \\ 0 & 0 & 0 & 0 & \mathbf{c}_{25} & 0 \\ 0 & 0 & 0 & 0 & 0 & \mathbf{c}_{36} \end{pmatrix} \begin{pmatrix} \vec{E}_x^2 \\ \vec{E}_y^2 \\ \vec{E}_z^2 \\ \vec{E}_z \vec{E}_x \\ \vec{E}_y \vec{E}_z \\ \vec{E}_x \vec{E}_y \end{pmatrix} \quad (2.42)$$

In case of RDP crystal,  $\vec{P}_{2w}^{NLS}$  in  $x$ ,  $y$  and  $z$  (optic) axis is derived as

$$\begin{aligned} P_x^{NLS}(2\mathbf{w}) &= \mathbf{c}_{14} E_z E_y \\ P_y^{NLS}(2\mathbf{w}) &= \mathbf{c}_{25} E_y E_x \\ P_z^{NLS}(2\mathbf{w}) &= \mathbf{c}_{36} E_x E_y \end{aligned} \quad (2.43)$$

In that incident beam having polarization of applied field in  $x$  and  $-y$  direction or  $[1\bar{1}0]$  respect to the crystallographic orientation, the nonlinear polarization inside the medium will grow along  $z$  direction or  $[001]$  direction whereas  $P_x^{NLS}(2\mathbf{w}) = P_y^{NLS}(2\mathbf{w}) = 0 = 0$  cause of  $E_z = 0$  by  $z$  axis as optic axis of the crystal.

$$P_z^{NLS}(2\mathbf{w}) = \mathbf{c}_{36} E_x E_y, \quad (2.44)$$

when  $E_x$  and  $E_y$  are the electric field of fundamental wave at each point inside the crystal with polarization in  $x$  and  $y$  direction.

Following (2.38), (2.39) and (2.44), the reflected SHI is proportional to the transmitted fundamental beam. In practice, it is very difficult to measure the quantities of transmitted fundamental beam inside the crystal. In order to achieve the

expression of reflected SHI in terms of fundamental wave, the linear Fresnel factor will be utilized:

$$P_z^{NLS}(\mathbf{2}\mathbf{w}) = \mathbf{C}_{36}^{NL} \mathbf{h} (F_T^L E_o)^2, \quad (2.45)$$

where  $\mathbf{h}$  is a geometrical factor that depends on the orientation of the fundamental field vector and nonlinear polarization component with respect to the crystallographic cubic axes of the RDP. The linear Fresnel factor  $F_T^L$  describes the changes of amplitude in the fundamental wave upon transmission at the crystal surface. If the incident wave with respect to the crystallographic cubic axes of the RDP crystal polarizes perpendicularly to the plane of incidence,  $F_{T,\perp}^L$  is given by

$$F_{T,\perp}^L = \frac{2 \cos \mathbf{q}_i}{\cos \mathbf{q}_i + \sin \mathbf{q}_{cr}(\mathbf{w}) \cos \mathbf{q}_s}, \quad (2.46)$$

where  $\mathbf{q}_{cr}(\mathbf{w})$  is the critical angle of incidence of the fundamental beam and is determined by using Shell's law as the relation of  $\mathbf{q}_R$ ,  $\mathbf{q}_S$  and  $\mathbf{q}_T$  with the refractive index. From figure 2.11, the wave vector in reflection,  $\vec{k}_{2w}^R$ ; inhomogeneous transmission,  $\vec{k}_{2w}^S$ ; and homogeneous transmission,  $\vec{k}_{2w}^T$ ; make angles of  $\mathbf{q}_R$ ,  $\mathbf{q}_S$  and  $\mathbf{q}_T$  to face normal. Using Snell's law and  $n = \sqrt{\epsilon}$ , then

$$n_{liq}^w \sin \mathbf{q}_i = n_{liq}^{2w} \sin \mathbf{q}_R = n_o^w \sin \mathbf{q}_S = n_e^{2w} \sin \mathbf{q}_T, \quad (2.47)$$

where  $n_{liq}(\mathbf{w})$  and  $n_{liq}(2\mathbf{w})$  are the refractive indices of optically denser liquid, 1-bromonaphthalene, for the fundamental laser and second-harmonic light, respectively.

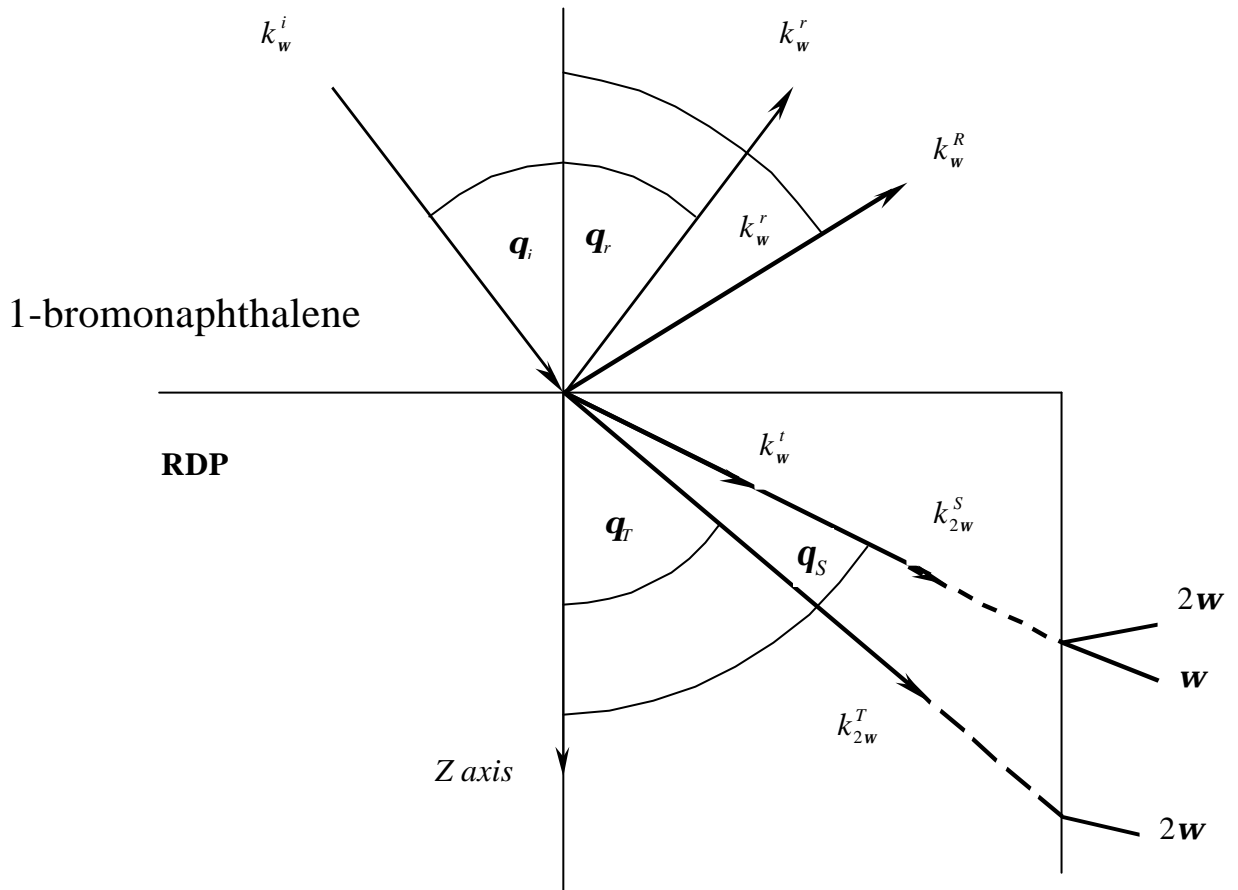


**Figure 2.11.** The propagated direction of the harmonic wave at the boundary of RDP crystal and 1-Bromonaphthalene liquid

The refractive indices without subscript refer to the RDP crystal, which is the negative uniaxial crystal, ( $n_o > n_e$ ). Its extraordinary refractive index,  $n_e^{2w}(\mathbf{q})$ , depends on the angle between incident wave and optic axis as

$$\frac{1}{[n_e^{2w}(\mathbf{q})]^2} = \frac{\cos^2 \mathbf{q}}{[n_o^{2w}]^2} + \frac{\sin^2 \mathbf{q}}{[n_o^{2w}(\mathbf{p}/2)]^2} \quad (2.48)$$

where  $n_o$  and  $n_e$  are the ordinary and extraordinary refractive indices. Here  $\theta$  is the angle between the optic axis of nonlinear crystal and the propagation vector  $\vec{k}_{2w}^T$ , as in figure 2.12.

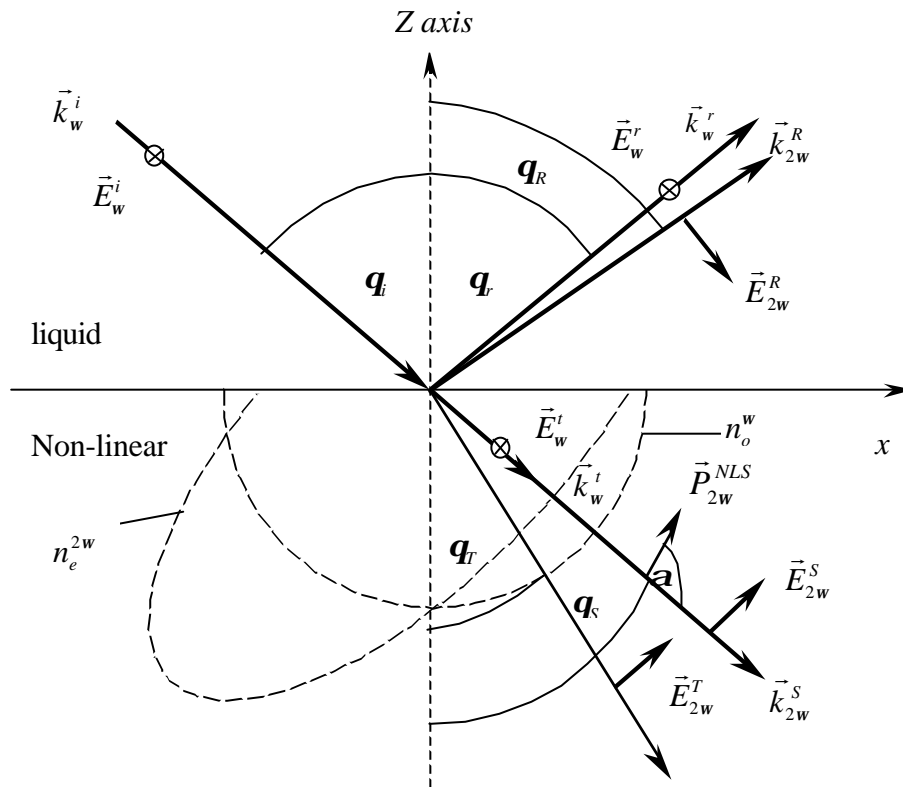


**Figure 2.12.** The geometry of the RDP refractive index of ellipsoid employed to investigate the reflected SHI.

In case of total reflection, the crystal is immersed in the higher-dense liquid, 1-bromonaphthalene, whose  $n_{liq}(\mathbf{w}) > n_o(\mathbf{w})$  and  $n_{liq}(\mathbf{w}) > n_o(\mathbf{w})$ . Thus the critical angle for  $\vec{k}_{2w}^S$  and  $\vec{k}_{2w}^T$  will be  $\mathbf{q}_w^{cr}$  and  $\mathbf{q}_{2w}^{cr}$ , respectively, and can be calculated from (2.49)

$$\begin{aligned}\sin \mathbf{q}_w^{cr} &= n_o^w / n_{liq}^w \text{ and} \\ \sin \mathbf{q}_{2w}^{cr} &= n_e^{2w} / n_{liq}^{2w}.\end{aligned}\quad (2.49)$$

According to (2.48), the  $F_{T,\perp}^L$  can be divided in another formula using  $n_i = \frac{n_o^w \sin \mathbf{q}_s}{\sin \mathbf{q}_i}$

$$\begin{aligned}F_{T,\perp}^L &= \frac{2 \sin \mathbf{q}_s \cos \mathbf{q}_i}{\sin \mathbf{q}_s \cos \mathbf{q}_i + \sin \mathbf{q}_i \cos \mathbf{q}_s} \\ &= \frac{2 \sin \mathbf{q}_s \cos \mathbf{q}_i}{\sin(\mathbf{q}_s + \mathbf{q}_i)}\end{aligned}\quad (2.50)$$

From all of the above, the reflected SHI with  $[1\bar{1}0]$  incident polarization passing the liquid through RDP crystal is given by (2.51) whereas the induced  $\vec{P}_{2w}^{NLS}$  lies in plane of incidence.

$$I_{2w}^R = \frac{c}{8p} \sqrt{\mathbf{e}_R} |E_o|^4 dd' (4p\mathbf{c}_{36}^{NL})^2 \mathbf{h}^2 |F_{T,\perp}^L|^4 |F_{R,\parallel}^{NL}|^2 \frac{\cos \mathbf{q}_R}{\cos \mathbf{q}_i} \quad (2.51)$$

However, the term  $\frac{c}{8p} \sqrt{\mathbf{e}_R} |E_o|^4 dd' (4p\mathbf{c}_{36}^m)^2 \mathbf{h}^2$  is constant for each crystal orientation and incident situation. So  $I^R(2w)$  will be treated as the relative magnitude as.

$$I_{2w}^R = |F_{T,\perp}^L|^4 |F_{R,\parallel}^{NL}|^2 \frac{\cos \mathbf{q}_R}{\cos \mathbf{q}_i} \quad (2.52)$$

### 2.3 Phase Matching in Second Harmonic Generation

To achieve the optimum SHG, the reflected SHI might be enhanced by choosing high nonlinear susceptibility and using high peak power of fundamental beam, as  $I_{2\omega}^R$  in (2.52). In this case, the RDP crystal is utilized because its  $\mathbf{c}^{NL}$  is approximately to  $\mathbf{c}^{NL}$  of KDP, which is widely used to generate the second harmonic wave. Besides, the phase matching technique (Maker et al., 1962; Giordmaine, 1962), would be advantageous, so that a fundamental ordinary wave and second harmonic extraordinary wave have the same propagating direction. The following elucidates this further

From

$$P_{2\omega}^{NLS} = \mathbf{c}_{ijk} (2\omega) E_j(\omega) E_k(\omega), \quad (2.53)$$

the  $P_{2\omega}^{NLS}$  induced inside the medium generates the second harmonic wave as

$$E_i(2\omega) = \mathbf{c}_{ijk}^{NL} E_j(\omega) E_k(\omega) \left\{ \frac{1 - \exp i(\Delta\vec{k} \cdot \vec{r})}{\Delta\vec{k}} \right\}, \quad (2.54)$$

where

$$\begin{aligned} \Delta\vec{k} &= \vec{k}(2\omega) - 2\vec{k}(\omega) \\ &= \frac{2\omega}{c} (n^{2\omega} - n^\omega) \end{aligned} \quad (2.55)$$

Then the intensity of SHG is given by

$$I^R(2\mathbf{w}) \propto E^T(\mathbf{w})^2 \left\{ \frac{1 - \exp i(\Delta\vec{k} \cdot \vec{r})}{\Delta\vec{k}} \right\}, \quad (2.54)$$

or

$$I^R(2\mathbf{w}) = [E^T(\mathbf{w})]^2 \left[ \frac{\sin^2\left(\frac{\Delta k}{2}\right)}{\left(\frac{\Delta k}{2}\right)^2} \right], \quad (2.55)$$

From (2.55) the optimization of SHI can be achieved by maximizing

$$\frac{\sin^2\left(\frac{\Delta k}{2} \cdot r\right)}{\left(\frac{\Delta k}{2}\right)^2} \text{ or phase factor term.}$$

The phase factor term is maximum when  $\mathbf{Dk}$  is zero. This condition is called phase matching as shown by

$$\mathbf{Dk} = \frac{2\mathbf{w}}{c} (n_e^{2\mathbf{w}} - n_o^{\mathbf{w}}) = 0. \quad (2.56)$$

To satisfy  $\mathbf{Dk} = 0$ , it is necessary that  $n_e^{2\mathbf{w}} = n_o^{\mathbf{w}}$ . This is referred to as index matching. Then SHI will be optimized. In a negative uniaxial crystal, RDP,  $n_o > n_e$ . The index surface at the fundamental frequency and the extraordinary index surface at the second harmonic are illustrated in figure 2.13.

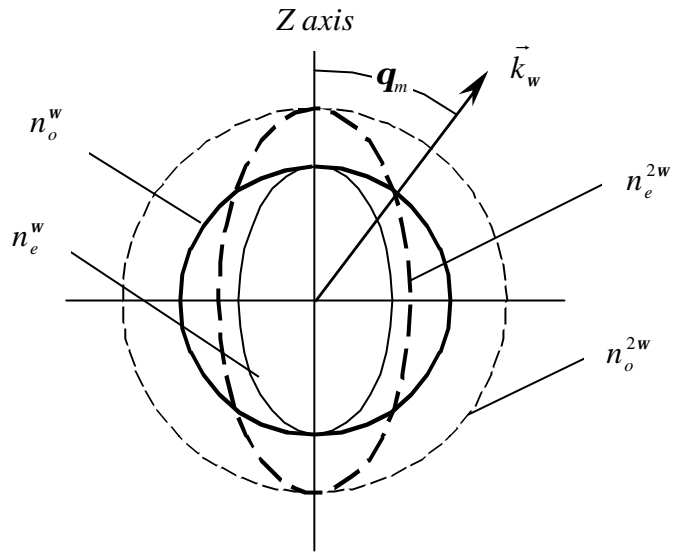


**Figure 2.13.** Geometry for phase matching in negative uniaxial crystal, Yariv (1989).

The angle between the intersection of each refractive indices and  $z$  axis is called phase matching angle, ( $\theta_m$ ). It can be derived from the index of ellipsoid of nonlinear medium.

$$\frac{1}{[n_e(\mathbf{w})]^2} = \frac{\cos^2 \mathbf{q}}{n_o^2} + \frac{\sin^2 \mathbf{q}}{n_e^2(\mathbf{p}/2)} \quad (2.57)$$

When  $n_e^{2w}(\mathbf{q}_m) = n_o^w$ , there is phase matching. Then (2.57) is rearranged for  $\mathbf{q}$

$m$  as

$$\mathbf{q}_m = \sin^{-1} \left[ \frac{(n_o^{2w})^{-2} - (n_o^w)^{-2}}{(n_o^w)^{-2} - (n_o^w)^{-2}} \right]^{1/2} \quad (2.58)$$

## 2.4 Nonlinear Brewster Angle, $q_i^{NB}$

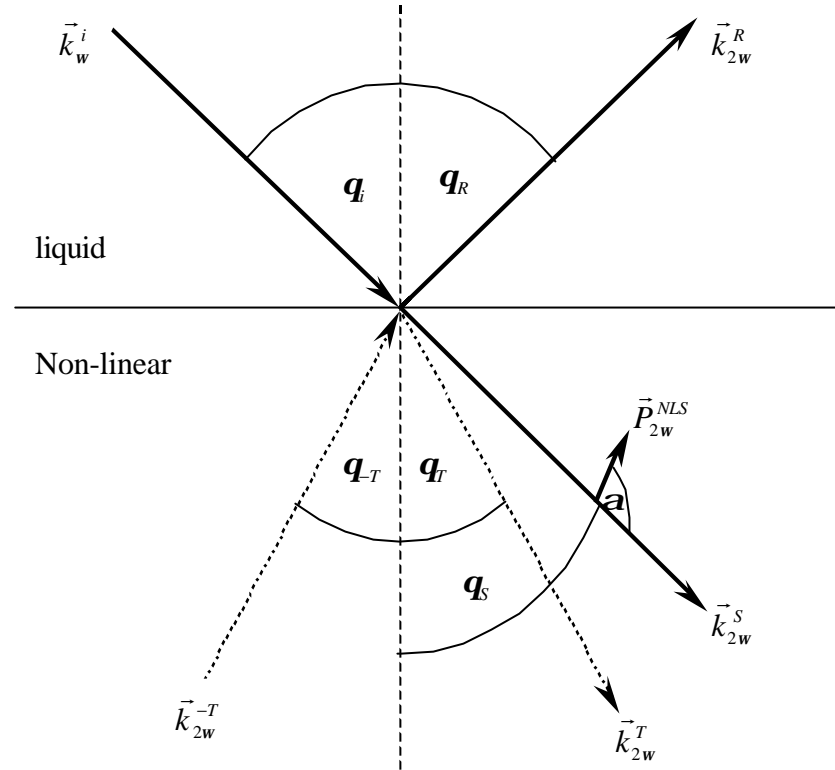


**Figure 2.14.** Geometry for existing nonlinear Brewster angle

Bloembergen and Pershan (1962) theory predicted the vanished reflected SHI that it would be occur at nonlinear Brewster angle ( $q_i^{NB}$ ). This is analogous to the Brewster angle in linear optics. However, the nonlinear Brewster angle can occur only when the  $\vec{P}_{2w}^{NLS}$  lies in then plane of incidence, for then reflected SHI will have vanished,  $I_{2w}^R = 0$ . The confirmations of  $q_i^{NB}$  were experimentally demonstrated by Bloembergen and Chang (1966); Lee and Bhanthumnavin (1976); Bhanthumnavin and Lee (1994). The value of  $q_i^{NB}$  is not unique, however. It depends on the crystallographic orientation and the polarization of the incident

polarization. The existence of the nonlinear Brewster angle is shown in figure 2.14. The condition for the occurrence of nonlinear Brewster angle mentioned above implies that the nonlinear polarization,  $P_{2w}^{NLS}$  is parallel to that direction of propagation in the nonlinear medium,  $\vec{k}^{-T}$ , which on refraction into the linear medium gives rise to the reflected ray in the direction  $\mathbf{q}_R$ . One may say  $P_{2w}^{NLS}$  is same direction of  $\vec{k}^{-T}$  and also lies in plane of incidence,  $\vec{k}^{-T} // \vec{P}_{2w}^{NLS} // \text{plane of incidence}$ . Therefore, the incident laser beam polarization is set so that the reflected second harmonic polarization lies in this plane. The mathematical interpretation for  $I_{2w}^R = 0$  is treated by

$$I_{2w}^R \propto |F_T|^4 |F_{R,11}^{NL}|^2 \frac{\cos \mathbf{q}_R}{\cos \mathbf{q}_j}. \quad (2.59)$$

Here  $I_{2w}^R = 0$ , whenever  $F_{R,11}^{NL} = 0$ , so that:

$$\sin(\mathbf{a} + \mathbf{q}_s + \mathbf{q}_T) = 0$$

or 
$$\mathbf{a} + \mathbf{q}_s + \mathbf{q}_T = n\mathbf{p} \quad (2.60)$$

where  $n = 0, 1, 2, 3, \dots$

By satisfying this condition,  $I_{2w}^R = 0$ , the nonlinear Brewster angle will be obtained from (2.60).

## CHAPTER III

### PROCEDURE

In this chapter, the procedure of theoretical study for reflected second harmonic generation (SHG) in RDP crystal is described in order to obtain results as explained in detail in the next chapter. In this study, an ultrashort pulsed laser is employed as a fundamental source for the incident light of frequency  $\omega$ . The negative uniaxial crystal rubidium dihydrogen phosphate (RDP) of point group  $\bar{4}2m$  is a nonlinear optical medium for SHG at frequency of  $2\omega$ . One feature of this study is phase matching at total reflection. Therefore, it is required an isotropic linear medium of an optically denser index of refraction so that total reflection from RDP crystal will be achieved. Furthermore, the computer program C<sup>++</sup> version 3.0 and Microsoft Excel version 7.0 are used for calculation of second harmonic intensity (SHI) as a function of incident angle  $\theta_i$ . Details of the procedure are described as follows.

#### 3.1 Ultrashort Pulse Laser

The study of reflected SHG from RDP at phase matching at total reflection and also the nonlinear Brewster angle ( $I_{2\omega}^R \rightarrow 0$ ) will require a proper coherent source: an ultrashort pulse laser with a pulsewidth in an order of Q-switched pulse or narrower. It is employed as the fundamental beam of  $\lambda = 900$  nm with polarization in  $[1\bar{1}0]$  direction with respect to the RDP crystallographic axes. Due to the property of RDP, the  $\vec{P}_{2\omega}^{NLS}$  will be in  $[001]$ , an optic axis. The advantage of an ultrashort pulse laser is that it has low energy of few millijoules. However, because of its short pulse duration, it has a very high peak power of greater than  $100 \text{ MW/cm}^2$ . This will be a very powerful excitation source for SHI when  $\mathbf{q}_i$  approaches the nonlinear Brewster angle whereby  $I_{2\omega}^R$  will rapidly decrease to null intensity.

### 3.2 Rubidium Dihydrogen Phosphate (RDP) Crystal

RDP is an anisotropic nonlinear optical medium, a negative uniaxial crystal of  $\bar{4}2m$  point group. It has two indices of refraction namely, ordinary index  $n_o$  and extraordinary index  $n_e$ , with  $n_o$  greater than  $n_e$ . Furthermore, the RDP crystal has real nonlinear susceptibility and so is transparent at both fundamental and second harmonic wavelengths. Therefore, there will be no absorption at frequencies  $\omega$  and  $2\omega$ . This transparency property enables the theoretical calculation and observation in the vicinity of nonlinear Brewster angle in the experiment for SHI to be enhanced. The value of  $n_o^{\omega}; n_o^{2\omega}; n_e^{\omega}(\mathbf{p}/2)$  and  $n_e^{2\omega}(\mathbf{p}/2)$  were calculated at wavelength of 900 nm and 450 nm and are given in appendix A

At  $\lambda = 900$  nm

$$n_o^w = 1.4965; \quad n_e^w = 1.4716.$$

At  $\lambda = 450$  nm

$$n_o^{2w} = 1.5160; \quad n_e^{2w} = 1.4857.$$

The phase matched condition requires  $n_o^w = n_e^{2w}$  whereby  $\vec{k}_{2w}^S$  and  $\vec{k}_{2w}^T$  travel in the same direction inside the RDP crystal. As the result, the enhancement of SHI ( $I_{2w}^R$ ) will reach its maximum value. According to the equation of index of ellipsoid at phase matched angle,  $\mathbf{q}_m$ , the  $\mathbf{q}_m$  can be found from the equation.

$$\frac{1}{[n_o^w]^2} = \frac{\cos^2 \mathbf{q}_m}{[n_o^{2w}]^2} + \frac{\sin^2 \mathbf{q}_m}{[n_e^{2w}(\mathbf{p}/2)]^2} \quad (3.1)$$

therefore

$$\mathbf{q}_m = \sin^{-1} \left\{ \frac{(n_o^w)^{-2} - (n_o^{2w})^{-2}}{[(n_e^{2w}(\mathbf{p}/2))^{-2} - (n_o^{2w})^{-2}]^{1/2}} \right\} \quad (3.2)$$

Upon substitution of appropriate value of  $n_o^w$ ;  $n_o^{2w}$ ;  $n_e^w(\mathbf{p}/2)$  and  $n_e^{2w}(\mathbf{p}/2)$  in (3.2), the value  $\mathbf{q}_m$  will be obtained as

$$\mathbf{q}_m = \sin^{-1} \left\{ \frac{(1.4965)^{-2} - (1.5160)^{-2}}{[(1.4857)^{-2} - (1.5160)^{-2}]^{1/2}} \right\}$$

Then

$$\mathbf{q}_m = 52.93^\circ \quad (3.3)$$

### 3.3 Liquid 1-Bromonaphthalene

Facilitating the condition of total reflection from RDP crystal requires an isotropic medium which occur naturally liquid form liquid. Liquid 1-bromonaphthalene is a good candidate due to its index of refraction  $n_{liq} > n_{RDP}$ . The liquid is an isotropic medium and has transparency properties at  $\lambda = 900$  nm and  $\lambda = 450$  nm. Furthermore, the liquid has high threshold damage for high peak laser pulses. Therefore, it is always stable under repeated incidence laser pulses. It also is noncorrosive and stable at room temperature. The 1-Bromonaphthalene vapor causes no health hazard to human. The indices of refraction at  $\lambda = 900$  nm and  $\lambda = 450$  nm are calculated by extrapolation with the help of Cauchy Formulas, (Jenkin and White, 1976):

$$n_{liq}^w = 1.693; \quad n_{liq}^{2w} = 1.6781.$$

Their calculation is given in appendix A. Since the laser pulse enters the uniaxial crystal RDP from the liquid of higher index of refraction, therefore, there are two angles of critical incidence (Bloembergen, Simon, and Lee, 1969); (Bhanthumnavin and Lee, 1990, 1994). The values of the two critical angles of incidence are

$$\begin{aligned}
\mathbf{q}_w^{cr} &= \sin^{-1} \left( \frac{n_o^w}{n_{liq}^w} \right) \\
&= \sin^{-1} \left( \frac{1.4965}{1.6335} \right) \\
&= 66.37^\circ
\end{aligned} \tag{3.4}$$

and

$$\begin{aligned}
\mathbf{q}_{2w}^{cr} &= \sin^{-1} \left( \frac{n_e^{2w}}{n_{liq}^w} \right) \\
&= \sin^{-1} \left( \frac{n_e^{2w}}{1.6952} \right)
\end{aligned} \tag{3.5}$$

### 3.4 Computer Program

In the study, the ultrashort pulse laser beam has polarization in  $[1\bar{1}0]$  direction with respect to RDP crystallographic axes. Due to the properties of  $\bar{4}2m$  point group possessed by the RDP crystal, the  $P_{2w}^{NLS}$  given by (2.44)

$$P_{2w}^{NLS} = \mathbf{c}_{36} E_x E_y, \tag{2.44}$$

will be in the  $z$ , optic axis or  $[001]$  direction. Furthermore, the study involves nonlinear Brewster angle at different  $\vec{P}_{2w}^R$  orientation, therefore, it is required that  $\vec{P}_{2w}^{NLS}$  must be in the plane of incidence (Bloembergen and Pershan, 1962). The equation given in chapter 2 for SHI in reflection is:

$$I_{2w}^R = \frac{c}{8\mathbf{p}} \sqrt{\mathbf{e}_R} |E_0|^4 dd' (4\mathbf{p}\mathbf{c}_{36}^{NL})^2 \mathbf{h}^2 |F_{T,\perp}^L|^4 |F_{R,\parallel}^{NL}|^2 \frac{\cos \mathbf{q}_R}{\cos \mathbf{q}_i} \tag{2.51}$$

where

$$F_{T,\perp}^L = \frac{2 \cos \mathbf{q}_i}{\cos \mathbf{q}_i + \sin \mathbf{q}_w^{cr} \cos \mathbf{q}_s}, \text{ and} \quad (2.46)$$

$$F_{R,\parallel}^{NL} = \frac{\sin \mathbf{q}_s \sin^2 \mathbf{q}_T \sin(\mathbf{a} + \mathbf{q}_s + \mathbf{q}_T)}{\mathbf{e}_R \sin \mathbf{q}_R \sin(\mathbf{q}_s + \mathbf{q}_T) \sin(\mathbf{q}_T + \mathbf{q}_R) \cos(\mathbf{q}_T - \mathbf{q}_s)}. \quad (2.39)$$

Since the terms  $\frac{c}{8\mathbf{p}} \sqrt{\mathbf{e}_R} |E_0|^4 dd'(4\mathbf{p}c_{36}^{NL})^2 \mathbf{h}^2$  in (2.51) of  $I_{2w}^R$  are treated as a constant in

the calculation for relative SHI,  $I_{2w}^R$ ,  $I_{2w}^R$  can be calculated from

$$I_{2w}^R = \mathbf{a} \left| F_{T,\perp}^L \right|^4 \left| F_{R,\parallel}^{NL} \right|^2 \frac{\cos \mathbf{q}_R}{\cos \mathbf{q}_i} \quad (2.52)$$

The computer program for calculation will involve equation (2.52). The C++ program and Microsoft Excel are utilized for calculation of  $I_{2w}^R$  as a function of  $\mathbf{q}_i$  and is displayed in a semi-logarithm graph as shown in chapter 4.

The flow chart concerning procedure and block diagram for calculation is shown in figure 3.1 as shown.

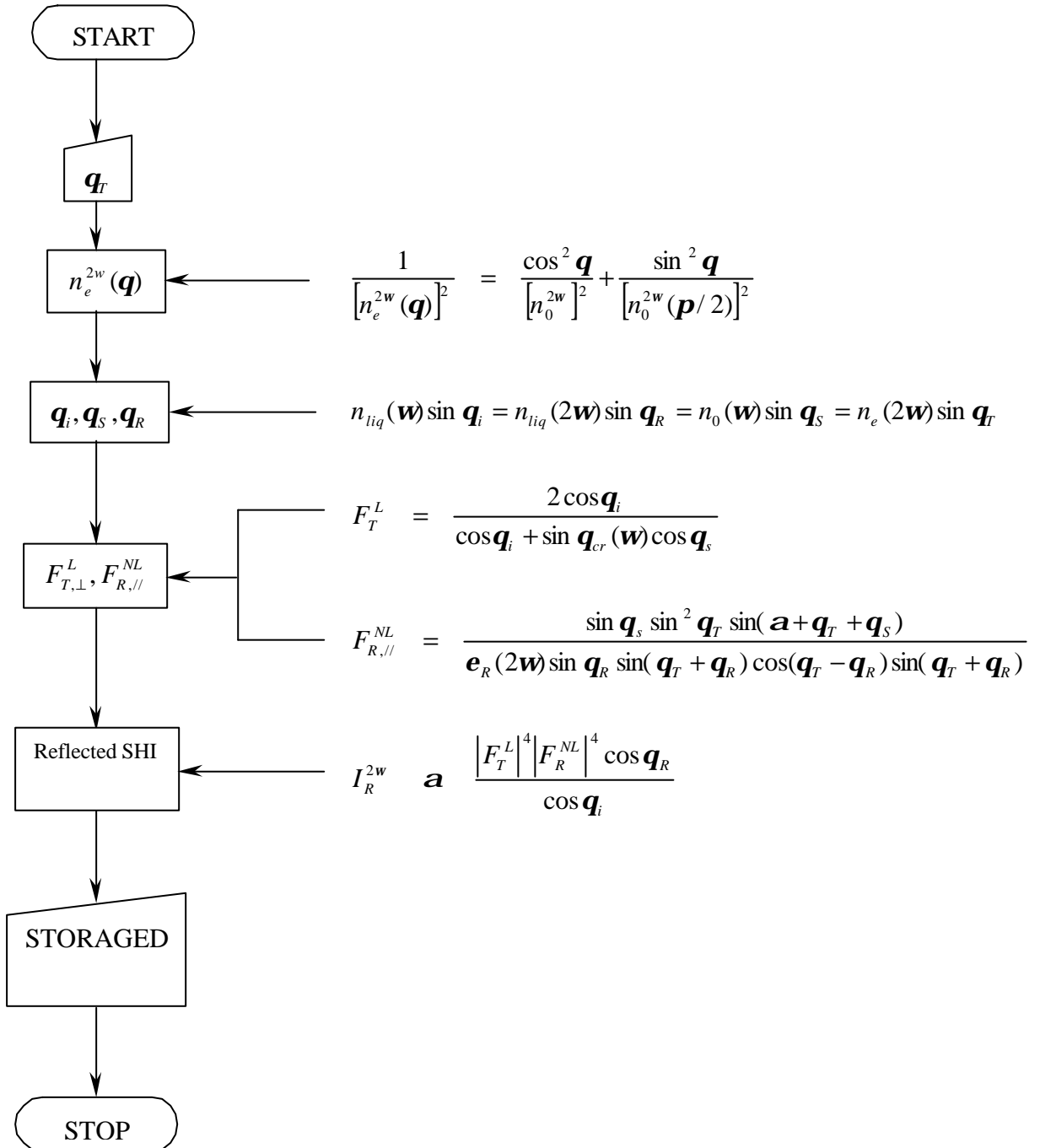


**Figure 3.1.** The flowchart for calculation of reflected second harmonic intensity.

## CHAPTER IV

### THEORETICAL RESULTS

In this chapter, results of the theoretical study of reflected second harmonic generation (SHG), using an ultrashort pulse laser as incident beam and RDP crystal immersed in 1-Bromonaphthalene, as the nonlinear crystal are described and analyzed as given below. The polarization of the incident laser beam is set at the  $[1\bar{1}0]$  direction and due to RDP crystal properties, the  $\vec{P}_{2\omega}^{NLS}$ , as a result, will be in the  $[001]$  direction. The results of this theoretical study lie in the reflected SHI at phase matched condition at total reflection,  $\mathbf{q}_i = \mathbf{q}_i^{cr}(\mathbf{w})$  and new nonlinear Brewster angles at different orientations of  $\vec{P}_{2\omega}^{NLS}$ .

#### 4.1 Phase Matched at Total Reflection

Theoretical study of reflected SHI,  $I_{2\omega}^R$ , at phase matched condition at total reflection is set up by arrangement of RDP crystal with  $\vec{P}_{2\omega}^{NLS}$  making the phase matched angle  $\mathbf{q}_m = 52.93^\circ$  with respect to the incident surface as shown in figure 4.1. There are two striking phenomena from this set up, namely,  $I_{2\omega}^R \rightarrow$  maximum value at

$\mathbf{q}_i = \mathbf{q}_i^{cr}(\mathbf{w}) = 63.37^\circ$  and  $I_{2w}^R \rightarrow$  minimum at nonlinear Brewster angle

$\mathbf{q}_i = \mathbf{q}_i^{NB} = 33.30^\circ$ . Results of this investigation are described in detail as follows.

#### 4.1.1 Phase matched SHI at Total Reflection

The result is shown in figure 4.1 where the incident angle lies in between  $50^\circ < \mathbf{q}_i < 75^\circ$ . From the graph in figure 4.1, one can see that when  $\mathbf{q}_i$  increases to the value of  $\mathbf{q}_i = \mathbf{q}_i^{cr}(\mathbf{w}) = 66.37^\circ$ ,  $I_{2w}^R$  will increase rapidly and reach maximum value at  $\mathbf{q}_i = \mathbf{q}_i^{cr}(\mathbf{w})$  where,  $\mathbf{q}_s = \mathbf{q}_t = 90^\circ$ , due to phase matching at total reflection.

Since

$$I_{2w}^R \propto |F_{T,\perp}^L|^4 |F_{R,\parallel}^{NL}|^2 \frac{\cos \mathbf{q}_R}{\cos \mathbf{q}_i} \quad (2.51)$$

and

$$F_{T,\perp}^L = \frac{2 \cos \mathbf{q}_i}{\cos \mathbf{q}_i + \sin \mathbf{q}_w^{cr} \cos \mathbf{q}_s} \quad (2.46)$$

at total reflection, then  $F_{T,\perp}^L \rightarrow 2$

Also since

$$F_{R,\parallel}^{NL} \propto \frac{\sin \mathbf{q}_s \sin^2 \mathbf{q}_t \sin(\mathbf{a} + \mathbf{q}_s + \mathbf{q}_t)}{\sin \mathbf{q}_R \sin(\mathbf{q}_t + \mathbf{q}_R) \cos(\mathbf{q}_i + \mathbf{q}_R) \sin(\mathbf{q}_t + \mathbf{q}_s)}, \quad (2.39)$$



$F_{R, //}^{NL} \rightarrow$  maximum value as  $\mathbf{q}_s$  and  $\mathbf{q}_t$  approach  $90^\circ$ . Therefore, for phase matched condition ( $n_o^w = n_e^{2w}$ ) at total reflection ( $\mathbf{q}_i = \mathbf{q}_i^{cr}(\mathbf{w})$ ), one get  $I_{2w}^R \rightarrow$  maximum value as shown in figure 4.1.

Note that the intensity of SHI,  $I_{2w}^R$  increases by  $10^7$  order of magnitude as  $\mathbf{q}_i$  varies between  $60^\circ < \mathbf{q}_i < 70^\circ$ .

#### 4.1.2 Nonlinear Brewster Angle at $\mathbf{q}_i = \mathbf{q}_i^{NB} = 33.30^\circ$

With the same orientation of  $\vec{P}_{2w}^{NLS}$  used for phase matching condition as indicated in figure 4.1, it is found out that as  $\mathbf{q}_i$  increases from  $20^\circ$  and approaches  $\mathbf{q}_i = \mathbf{q}_i^{NB} = 33.30^\circ$ ,  $I_{2w}^R$  decreases rapidly. The minimum  $I_{2w}^R$  is at  $\mathbf{q}_i = \mathbf{q}_i^{NB} = 33.30^\circ$  so that as  $\mathbf{q}_i > \mathbf{q}_i^{NB}$ ,  $I_{2w}^R$  increases to higher value. Therefore, from figure 4.1 in the region of  $20^\circ < \mathbf{q}_i < 45^\circ$ , there is a dip of  $I_{2w}^R$  at  $\mathbf{q}_i^{NB} = 33.30^\circ$  and dynamical range of  $I_{2w}^R$  in this region is about  $10^{12}$ . The analysis for  $I_{2w}^R \rightarrow$  minimum value at  $\mathbf{q}_i = \mathbf{q}_i^{NL} = 33.30^\circ$  can be given as follows.

Since  $I_{2w}^R \propto |F_{R, //}^{NL}|^2$ , and

$$F_{R, //}^{NL} = \frac{\sin \mathbf{q}_S \sin^2 \mathbf{q}_T \sin(\mathbf{a} + \mathbf{q}_S + \mathbf{q}_T)}{\sin \mathbf{q}_R \sin(\mathbf{q}_T + \mathbf{q}_R) \cos(\mathbf{q}_T - \mathbf{q}_R) \sin(\mathbf{q}_T + \mathbf{q}_S)}, \quad (2.39)$$

$$F_{R, //}^{NL} \rightarrow 0, \text{ if } \mathbf{a} + \mathbf{q}_S + \mathbf{q}_T = 0, \mathbf{p}, 2\mathbf{p}, \dots$$

From figure 4.1, it is clear that

$$\mathbf{a} + \mathbf{q}_S = 360^\circ - \mathbf{q}_T$$

Therefore,  $\mathbf{a} + \mathbf{q}_S + \mathbf{q}_T = 360^\circ = 2\mathbf{p}$ . This will result in  $\sin(\mathbf{a} + \mathbf{q}_S + \mathbf{q}_T) = 0$  and as a consequence  $I_{2w}^R$  in (2.51) will be zero (minimum).

Summarizing, the orientation of  $\vec{P}_{2w}^{NLS}$  in this situation, as indicated in figure 4.1 will result in  $I_{2w}^R \rightarrow$  maximum value at  $\mathbf{q}_i = \mathbf{q}_i^{NB} = 66.37^\circ$  and  $I_{2w}^R \rightarrow$  minimum value at  $\mathbf{q}_i = \mathbf{q}_i^{NL} = 33.30^\circ$ . The total dynamical range of  $I_{2w}^R$  in the region  $20^\circ < \mathbf{q}_i < 75^\circ$  will be in the order of  $10^{19}$ . Furthermore, the results agree very well to the theoretical and experimental work of SHG in KDP crystal of the same situation, Bhanthumnavin and Lee (1990, 1994).

## 4.2 Nonlinear Brewster Angles

In this section, results of theoretical investigation for nonlinear Brewster angle will be presented in accordance with new different orientations of  $\vec{P}_{2w}^{NLS}$ . There are two nonlinear Brewster angles at  $\mathbf{q}_i = \mathbf{q}_i^{NB} = 0^\circ$  and  $\mathbf{q}_i = \mathbf{q}_i^{NB} = \mathbf{q}_{2w}^{cr} = 68.14^\circ$ , respectively. The detailed analysis is given as follows.

#### 4.2.1 Nonlinear Brewster Angle at $\mathbf{q}_i = \mathbf{q}_i^{NB} = 0^\circ$

The RDP crystal in this situation is cut in such a way that  $\vec{P}_{2w}^{NLS}$  which is in [001] direction, lies along face normal as shown in figure 4.2. According to this crystallographic set up of  $\vec{P}_{2w}^{NLS}$ , one will find a striking phenomena, in contrast to general expectation, that  $I_{2w}^R \rightarrow \text{minimum}$  at  $\mathbf{q}_i = \mathbf{q}_i^{NB} = 0^\circ$ . Thus means the nonlinear Brewster angle occurs at normal incident angle,  $\mathbf{q}_i = 0^\circ$ . This is in contrast to the general understanding that whenever fundamental laser beam is normally incident on a nonlinear crystal, there will be reflected SHI coming out. The reason for  $I_{2w}^R$  decreases to minimum value at  $\mathbf{q}_i = \mathbf{q}_i^{NB} = 0^\circ$  is following

$$\text{Since, } F_{R,II}^{NL} = \frac{\sin \mathbf{q}_S \sin^2 \mathbf{q}_T \sin(\mathbf{a} + \mathbf{q}_S + \mathbf{q}_T)}{\sin \mathbf{q}_R \sin(\mathbf{q}_T + \mathbf{q}_R) \cos(\mathbf{q}_T - \mathbf{q}_R) \sin(\mathbf{q}_S + \mathbf{q}_T)},$$

by applying generalized Snell's law at  $\mathbf{q}_i = 0^\circ$ , we will get  $\mathbf{q}_s = \mathbf{q}_r = 0^\circ$ . Therefore,

$$F_{R, //}^{NL} = 0,$$

and as a consequence

$$I_{2w}^R \mathbf{a} |F_{R, //}^{NL}|^2 = 0, \quad \text{as well.}$$

From figure 4.2, one can see that the variation of  $I_{2w}^R$  in the vicinity of  $\mathbf{q}_i = 0^\circ$  is about  $10^{14}$  order of magnitude.

#### 4.2.2 Nonlinear Brewster Angle at $\mathbf{q}_i = \mathbf{q}_i^{NB} = \mathbf{q}_{2w}^{cr} = 68.14^\circ$

Another nonlinear Brewster angle is investigated for the case of  $\vec{P}_{2w}^{NLS}$  lying along the incident surface of RDP crystal as shown in figure 4.3. This situation is corresponding to the occurrence of nonlinear Brewster angle at total reflection at  $\mathbf{q}_i = \mathbf{q}_{2w}^{cr} = 68.14^\circ$ . It is well understood that in case of non-phase matching at total reflection, there will be two critical angles of incidence (Bloembergen, Simon, and Lee, 1969); (Bhanthumnavin and Lee, 1990,1994). For this situation a nonlinear Brewster angle  $\mathbf{q}_i^{NB}$  occurs at  $\mathbf{q}_i^{NB} = \mathbf{q}_{2w}^{cr}$ .

The analysis of the occurrence of  $\mathbf{q}_i^{NB} = \mathbf{q}_{2w}^{cr} = 68.14^\circ$  can be given as follows.

$$\text{Since } F_{R, //}^{NL} = \frac{\sin \mathbf{q}_S \sin^2 \mathbf{q}_T \sin(\mathbf{a} + \mathbf{q}_S + \mathbf{q}_T)}{\sin \mathbf{q}_R \sin(\mathbf{q}_T + \mathbf{q}_R) \cos(\mathbf{q}_T - \mathbf{q}_R) \sin(\mathbf{q}_S + \mathbf{q}_T)},$$

$$F_{R, //}^{NL} \rightarrow 0, \text{ if } \mathbf{a} + \mathbf{q}_S + \mathbf{q}_T = 0, \mathbf{p}, 2\mathbf{p}, \dots$$

For this situation, shown in figure 4.3, it is clear that when  $\mathbf{q}_i = \mathbf{q}_{2w}^{cr} = 68.14^\circ$ , we will get  $\mathbf{q}_T = 90^\circ$  and therefore,  $\mathbf{a} + \mathbf{q}_S + \mathbf{q}_T = 270^\circ + 90^\circ = 2\mathbf{p}$  and consequently

$$\sin(\mathbf{a} + \mathbf{q}_T + \mathbf{q}_S) = 0. \text{ This will result in } I_{2w}^R \mathbf{a} \left| F_{R, //}^{NL} \right|^2 = 0.$$

It can be analyzed from another point of view that, according to BP theory, the nonlinear Brewster angle will occur when  $\vec{P}_{2w}^{NLS} // \vec{k}^{-T}$  vector. For this case,  $\vec{k}^{-T}$  is in

the direction along the incident face of RDP crystal. In other words, it is in the same direction as  $\vec{P}_{2w}^{NLS}$ . Therefore, the nonlinear Brewster angle prevails for this situation where  $\mathbf{q}_i = \mathbf{q}_i^{NL} = \mathbf{q}_{2w}^{cr}$ . This situation is interesting that  $I_{2w}^R \rightarrow$  minimum at total reflection in contrast to the situation in section 4.1 where  $I_{2w}^R \rightarrow$  maximum value at total reflection. This contrast can be explained and understood in view that the  $P_{2w}^{NLS}$  of the two cases are in different orientation despite of  $\mathbf{q}_i = \mathbf{q}_w^{cr}$ . It is observed that, as in figure 4.3, the dynamical range of  $I_{2w}^R$  in the vicinity of  $65^\circ < \mathbf{q}_i < 70^\circ$  is about  $10^{11}$  order of magnitude.

### 4.3 Investigation for a Definite Orientation of $\vec{P}_{2w}^{NLS}$ when $\mathbf{q}_i^{NL} = 30^\circ$ is Specified

It is interested to perform a theoretical investigation for a particular orientation of  $\vec{P}_{2w}^{NLS}$  of RDP crystal when a definite nonlinear Brewster angle,  $\mathbf{q}_i^{NB}$ , is expected. For this case,  $\mathbf{q}_i^{NB}$  is specified to be at  $\mathbf{q}_i = 30^\circ$ . According to a theoretical calculation as given in appendix B, it is found out that  $\vec{P}_{2w}^{NLS}$  must be in the plane of incidence and makes an angle of  $56.77^\circ$  to the incident surface of RDP crystal as shown in figure 4.4. At this orientation of  $\vec{P}_{2w}^{NLS}$ , it is theoretical predicted that  $\mathbf{q}_i^{NB}$  will be at  $\mathbf{q}_i = 30^\circ$ . The analysis, besides that given in the appendix B. is following.

Since  $I_{2w}^R \mathbf{a} |F_{R, //}^{NL}|^2$ , and

$$F_{R, //}^{NL} = \frac{\sin \mathbf{q}_s \sin^2 \mathbf{q}_T \sin(\mathbf{a} + \mathbf{q}_s + \mathbf{q}_T)}{\sin \mathbf{q}_R \sin(\mathbf{q}_T + \mathbf{q}_R) \cos(\mathbf{q}_T - \mathbf{q}_R) \sin(\mathbf{q}_T + \mathbf{q}_s)}, \quad (2.39)$$

$F_{R, //}^{NL} \rightarrow 0$ , if  $\mathbf{a} + \mathbf{q}_s + \mathbf{q}_T = 0, \mathbf{p}, 2\mathbf{p}, \dots$

According to figure B.1, it is found that  $\mathbf{a} + \mathbf{q}_s = 360^\circ - \mathbf{q}_T$ , therefore  $\mathbf{a} + \mathbf{q}_s + \mathbf{q}_T = 360^\circ$  and as a consequence  $\sin(\mathbf{a} + \mathbf{q}_s + \mathbf{q}_T) = 0$ . This will lead to

$F_{R, //}^{NL} = 0$ , and  $I_{2w}^R \mathbf{a} |F_{R, //}^{NL}|^2 = 0$  as well. Since  $\mathbf{q}_r = 90^\circ - 56.77^\circ = 33.23^\circ$ , by using the generalized Snell's law, we find that

$$\mathbf{q}_i = \sin^{-1} \left( \frac{n_e^{2w} \sin \mathbf{q}_r}{n_{liq}^w} \right)$$

Since we have  $n_o^w = n_e^{2w} (\mathbf{q} = 2 \times 33.23^\circ = 66.46^\circ) = 1.4904$

Therefore

$$\mathbf{q}_i^{NB} = \sin^{-1} \left[ \frac{1.4904 \sin(33.23^\circ)}{1.6335} \right] = 30^\circ.$$

From this situation, it is remarkable that a nonlinear Brewster angle can be specified at any given value where  $0 < \mathbf{q}_i^{NB} < 90^\circ$  corresponding to a calculated orientation of  $\vec{P}_{2w}^{NLS}$  as indicated in appendix B. Again, a dynamical range of  $I_{2w}^R$  of this case is in another of  $10^{12}$ .

## CHAPTER V

### DISCUSSION AND CONCLUSIONS

Since 1961, there has been many nonlinear optical experiments carried out in various situations. Second harmonic generation in reflection was first performed by Bloembergen and Ducuing (1962) from GaAs. Bloembergen and Lee (1966) performed phase matched at total reflection from KDP crystal and as a consequence Lee and Bhanthumnavin (1976), Bhanthumnavin and Lee (1990, 1994), theoretically and experimentally studied SHG at total reflection and also discovered a new nonlinear Brewster angle from KDP which is a  $\bar{4}2m$  point group crystal.

In this theoretical study, RDP crystal which has the same point group  $\bar{4}2m$  as of KDP crystal, is employed as a nonlinear medium. The ultrashort pulse laser is used as a fundamental beam of incidence at  $\lambda = 900$  nm and the second harmonic light of  $\lambda = 450$  nm is generated and many nonlinear Brewster angles are predicted in accordance to the orientation of  $\vec{P}_{2w}^{NLS}$  of RDP crystal. New nonlinear Brewster angles are found to be at  $\mathbf{q}_i = 0^\circ$ ;  $\mathbf{q}_i = 30^\circ$ ;  $\mathbf{q}_i = 33.30^\circ$  and  $\mathbf{q}_i = \mathbf{q}_w^{cr} = 68.14^\circ$ . The occurrence of many nonlinear Brewster angles,  $\mathbf{q}_i^{NB}$ , depend on the orientation of  $\vec{P}_{2w}^{NLS}$  which is in [001] direction. The summary of relationship of  $\mathbf{q}_i^{NB}$  and the orientation of  $\vec{P}_{2w}^{NLS}$  is given in a table 5.1 below.

**Table 5.1** Summary of nonlinear Brewster angles corresponding to various orientation of

$$\vec{P}_{2\omega}^{NLS}$$

INCLINATION OF $\vec{P}_{2\omega}^{NLS}$	$\mathbf{q}_i^{NL}$	REFLECTED SHI	
		Maximum	Minimum
1) $\vec{P}_{2\omega}^{NLS}$ lies along face normal (figure 4.2)	$0^\circ$	-	Minimum
2) $\vec{P}_{2\omega}^{NLS}$ makes an angle of $56.70^\circ$ to the crystal surface (figure 4.4)	$30^\circ$	-	Minimum
3) $\vec{P}_{2\omega}^{NLS}$ makes an angle of $52.93^\circ$ -phase matched condition (figure 4.1)	$33.30^\circ$	Maximum at $\mathbf{q}_i = \mathbf{q}_i^{cr}(\omega) = 66.37^\circ$	Minimum at $\mathbf{q}_i = 33.30^\circ$
4) $\vec{P}_{2\omega}^{NLS}$ lies along crystal surface (figure 4.3)	$68.41^\circ$	-	Minimum at $\mathbf{q}_i = \mathbf{q}_i^{cr}(2\omega) = 68.41^\circ$

Phase matching at total reflection, which means when  $\mathbf{q} = \mathbf{q}_i^{cr}$ , the critical angle of incidence, can obtain SHI at the maximum value ( $I_{2w}^R \rightarrow \text{maximum}$ ). This result is shown in figure 4.1. In this situation one also gets minimum  $I_{2w}^R$  which is a nonlinear Brewster condition at  $\mathbf{q}_i = \mathbf{q}_i^{NB} = 33.30^\circ$  as shown in figure 4.1. It is interesting that, on a second harmonic generation (SHG) point of view, one can produce SHI with a very large dynamical range of  $10^{24}$  orders of magnitude when  $\mathbf{q}_i$  is in between  $25^\circ$  to  $70^\circ$  as shown in figure 4.1.

In this study, not only are new nonlinear Brewster angles predicted from RDP crystal by using a new wavelength of laser at 900 nm as incident beam but also two striking phenomena are worth pointing out. The first is when  $\vec{P}_{2w}^{NLS}$  lies along face normal as shown in figure 4.2. In this situation we obtain nonlinear Brewster angle  $\mathbf{q}_i = \mathbf{q}_i^{NB} = 0^\circ$ . This means that there is no  $I_{2w}^R$  at  $\mathbf{q}_i = 0^\circ$ . It is contrary to a general understanding that, when an incident beam of laser is incident normally to a nonlinear optical medium, it is expected to generate reflected and transmitted SHI coming out along face normal direction, but obtain  $I_{2w}^R = 0$  at  $\mathbf{q}_i = 0^\circ$ , a nonlinear Brewster angle, instead. Therefore, this result is a confirmation of the Bloembergen and Pershan (BP) theory that the SHG is dependent on polarization of the incident beam as well as the orientation of  $\vec{P}_{2w}^{NLS}$  of the crystal. The result of this situation (as shown in figure 4.2) and table 5.1 agrees very well to the previous experiment of reflected SHG from KDP (of the same point group of  $\bar{4}2m$ ), (Bhanthumnavin and Lee, 1990, 1994).

The second striking phenomena is when  $\vec{P}_{2w}^{NLS}$  makes an angle of phase matching,  $\mathbf{q}_m = 52.93^\circ$  to the incident surface of the RDP crystal, as shown in figure 4.3. For this situation, one gets phase matched SHG at total reflection. This means that under this situation  $I_{2w}^R \rightarrow$  maximum value at  $\mathbf{q}_i = \mathbf{q}_i^{cr}(\mathbf{w}) = 66.37^\circ$ . It can be concluded that one can get maximum value of  $I_{2w}^R$  at total reflection from RDP crystal. However, in contrast, if one carefully examines the situation as shown in figure 4.3, one will see that at total reflection where  $\mathbf{q}_i = \mathbf{q}_i^{cr}(\mathbf{w})$ ,  $I_{2w}^R \rightarrow 0$ . This is a nonlinear Brewster angle. The situation of  $I_{2w}^R \rightarrow 0$  at total reflection is called the occurrence of nonlinear Brewster angle at total reflection. By comparing situations as shown in figure 4.1 and figure 4.3, one will see that they are in contradiction, despite of the same situation of total reflection,  $\mathbf{q}_i = \mathbf{q}_i^{cr}(\mathbf{w}) = 66.37^\circ$ , at which for one case  $I_{2w}^R$  is maximum and for another case of the same  $\mathbf{q}_i$ ,  $I_{2w}^R$  is minimum. The contradiction of the two cases can be explained by Bloembergen and Pershan (BP) Theory that, despite of the two cases sharing the same situation of total reflection, they give the contrasting results of  $I_{2w}^R$  as indicated in table 5.1 (item 3 and 4). Therefore, one can conclude that at total reflection  $I_{2w}^R$  will always greater than zero value. This is the beauty of the BP theory.

Furthermore, another striking result from this theoretical study is that by knowing the crystal point group of the nonlinear crystal i.e.  $\bar{4}2m$  as of RDP crystal by making crystal cut that will dictate the orientation of  $\vec{P}_{2w}^{NLS}$  and together with the polarization of laser beam, one can get any nonlinear Brewster angle corresponding to the definite orientation of  $\vec{P}_{2w}^{NLS}$

provided there is a fixed polarization of incident laser beam. This situation is shown in figure 4.4 and the calculation for orientation of  $\vec{P}_{2w}^{NLS}$  when  $\mathbf{q}_i = \mathbf{q}_i^{NB} = 30^\circ$  as indicated in appendix B. This result will lead us to an application whenever one wants  $I_{2w}^R \rightarrow 0$  at a particular  $\mathbf{q}_i = \mathbf{q}_i^{NB}$  of a certain crystal of  $\bar{4}2m$  point group. This situation can be used as an “optical switch” in the future.

Since this study is theoretical by nature, it is worthwhile to suggest an experimental preparation for verification of this theoretical prediction as follows.

- 1) The ultrashort pulsed laser system of Q-switched type or picosecond or femtosecond type is needed in order to produce a high peak power of at least  $100 \text{ MW/cm}^2$ . This will enhance SHG in vicinity of nonlinear Brewster angle where  $I_{2w}^R \rightarrow 0$ .
- 2) The RDP crystal, a nonlinear optical medium of  $\bar{4}2m$ , must be prepared and cut precisely in order to get a very definite orientation of  $\vec{P}_{2w}^{NLS}$  for the case of phase matched conditions and for nonlinear Brewster condition. It is strongly emphasized that the surface smoothness of the crystal must be in the order of at least  $\lambda/10$  in order to avoid interference of reflected SHI coming out of the crystal.
- 3) An isotropic optically denser fluid of 1-Bromonaphthalene is necessary to ensure the occurrence of total reflection from RDP crystal.

- 4) A very sensitive system for detection of SHI at  $\lambda = 450$  nm is required, since the SHI at the vicinity of nonlinear Brewster is very low. Therefore, a photomultiplier must have at least 10 dynodes in order to detect a very low-level signal of SHI.
- 5) There must be an optical filtering system composed of a neutral density filter, a spectral filter of a very narrow bandwidth centered at 450 nm together with polarizer and analyzer in order to discriminate the “spurious signal” of random polarization. An oscilloscope of a very fast rise time of at least  $10^{-9}$  second in order to handle the ultrafast laser pulse is also needed.

In conclusion, this theoretical study of reflected SHG from RDP by phase matching at total reflection as well as finding new nonlinear Brewster angles at different orientation of  $\vec{P}_{2w}^{NLS}$  agree very well to the theoretical and experimental study for the case of KDP crystal of the same point group of  $\bar{4}2m$ , Bhanthumnavin and Lee (1990, 1994); Lee and Bhanthumnavin (1976). This theoretical study will serve as an extension of Bloembergen and Pershan (BP) theory to another nonlinear crystal with different orientation of  $\vec{P}_{2w}^{NLS}$  corresponding to the assigned  $\mathbf{q}_i^{NB}$  is demonstrated and it can be used as an application for future “optical switch”. Suggestion for the application of the future “optical switch” can be given as follow. Since  $I_{2w}^R$  vanishes very fast to zero value when  $\mathbf{q}_i$  is in a vicinity of  $\mathbf{q}_i^{NB}$ ,

therefore, we can set up a diode pumped ultrashort pulse laser system of high peak power and let the laser beam incident on the RDP or  $\overline{42m}$  point group crystals at the  $\mathbf{q}_i = \mathbf{q}_i^{NB}$ . As a consequent, upon reflection  $I_{2w}^R = 0$  at the photomultiplier (detector). When the incident laser, which is mounted on a system which is required to be on a very precise location is moved by a minute lateral displacement, it will result in the displacement of the incident laser beam at  $\mathbf{q}_i \neq \mathbf{q}_i^{NB}$  resulting in increasing of  $I_{2w}^R$ . The photomultiplier will register and send a signal to a connected circuit. The circuit will be activated and acts as a turned on switch.

## REFERENCES

- Bhanthumnavin, V. and Ampole, N. (1990). Theoretical prediction of nonlinear Brewster angle in ADP. **Microwave and Optical Technology Letters.** (3); 239.
- Bhanthumnavin, V. and Lee, C.H. (1994). Optical second-harmonic generation of oblique incident light in transmission in potassium phosphate crystal. **J. Appl. Phys.** (75); 3294.
- Bhanthumnavin, V. and Lee, C.H. (1994). Optical second-harmonic generation at total reflection in potassium dihydrogen phosphate crystal. **Phys. Rev. A.** (50); 2579.
- Bloembergen, N. and Pershan, P.S. (1962). Light wave at the boundary of nonlinear media. **Phys. Rev.** (28); 600.
- Bloembergen, N. and Lee, C.H. (1966). Total reflection on second-harmonic generation. **Phys. Rev. Lett.** (19); 835.
- Bloembergen, N., Simon, H.J. and Lee, C.H. (1969). Total reflection phenomena in second-harmonic generation of light. **Phys. Rev.** (181); 1261.
- Chang, R. K. and Bloembergen, N. (1996). Experimental verification of the laws for the reflected intensity of second-harmonic light. **Phys. Rev.** (144); 775.
- Dmitriev, V. G., Gurzadyan, G. G. and Nikogosyan D. N. (1991). **Handbook of nonlinear optical crystals.** U.S.A.: Springer-Verlag.

- Ducuing, J. and Bloembergen, N. (1963). Observation of reflected light harmonic at the boundary of piezoelectric crystals. **Phys. Rev. Lett.** (10); 476.
- Franken, P. A., Hill, A. E., Peters, C. W., and Weinreich, G. (1961). Generation of optical harmonic. **Phys. Rev.** (127); 1918.
- Giordmaine, J. A., 1962, Mixing of Light Beams in Crystal. **Phys. Rev. Lett.** (8); 19.
- Hecht, E.(1987). **Optics (2<sup>rd</sup> ed.)**. U.S.A.: Addison-Wesley Publishing company.
- Jenkins, F. A. and White, H. E. (1976). **Fundamentals of Optics 4<sup>th</sup> ed.** McGraw-hill., Singapore.
- Lee, C. H. and Bhanthumnavin, V. (1976). Observation of nonlinear Brewster angle in KDP. **Opt. Comm.** (18).
- Maimann, T. H. (1960). Stimulated optical radiation in ruby. **Nature.** (187); 493.
- Maker, P. D., Terhune, R. W., Nisenoff M. and Savage C. M. (1962). Effects of dispersion and focusing on the production of optical harmonics. **Phys. Rev. Lett.** (8); 21.
- Nye, J. F. (1976). **Physical properties of crystal.** London: Oxford University Press.
- Suripon, U. and Bhanthumnavin, V. (1999). The theoretical prediction of nonlinear Brewster angle in a potassium dihydrogen phosphate (KDP) crystal. **25<sup>th</sup> congress on science and technology of Thailand, The Science Society of Thailand**, Naresuan University and Chulalongkorn University, 20-22 October 1999, Pitsanuloke.
- Vendeyen, J. T. (1995). **Laser Electronics (3<sup>th</sup> ed.)**. U.S.A: Printice-Hall International
- Yariv, A. (1991). **Optical Electronics (4<sup>th</sup> ed.)**. Philadelphia: Saunder College Publishing.

# **APPENDIXES**

## APPENDIX A

### THE CALCULATION FOR REFRACTIVE INDICES

In order to achieve the investigation of reflected second harmonic intensity as a function of incident angle, the refractive indices of higher-denser liquid, 1-Bromonaphthalene and a negative uniaxial crystal, RDP crystal, immersed in the liquid will be utilized by means of a generalized Snell's law, (Bloembergen and Pershan, 1962). Both of its refractive indices are actually dependent on the wavelength or frequency propagating inside the medium. The calculation for refractive indices of RDP crystal and 1-Bromonaphthalene can be obviously treated by using dispersive equations, (Dmitriev, Gurzadyan and Nikogosyan, 1991) and Cauchy's equation, (Jenkins and White, 1976), respectively.

#### A.1 The Calculation for indices of refraction of RDP Crystal

The computation for refractive indices of RDP crystal can be obtained as wavelength dependence by (A.1).

$$(n_o)^2 = 2.249885 + \frac{3.688005I^2}{I^2 - 127.1998253} + \frac{0.01056}{I^2 - 0.007780475} \quad (\text{A.1})$$

and

$$(n_e)^2 = 2.159913 + \frac{0.988431I^2}{I^2 - 127.692938} + \frac{0.0009515}{I^2 - 0.00847799}, \quad (\text{A.2})$$

where  $n_o$  and  $n_e$  are the ordinary and extraordinary refractive indices, respectively.

By substitution into (A.2), the indices of refraction at  $I = 450$  and  $900$  nm are achieved as follows.

At  $I = 900$  nm.,

$$\begin{aligned} n_o &= 1.4965 \\ n_e &= 1.4716 \end{aligned}$$

At  $I = 450$  nm.,

$$\begin{aligned} n_o &= 1.4965 \\ n_e &= 1.4716 \end{aligned}$$

**Table A.1.** Changes in refractive indices of RDP crystal with a wavelength range 0.266-1.064  $\mu\text{m}$ .

$\lambda$ [ $\mu\text{m}$ ]	$n_o$	$n_e$
0.266	1.5542	1.5206
0.355	1.583	1.4967
0.532	1.5100	1.4807
1.064	1.4920	1.4695

By comparison to the other typical values of refractive indices as shown, the RDP refractive indices are seen to be reasonable. As the result, the calculated refractive indices of RDP crystal at  $\lambda = 450$  and  $900$  nm make senses.

## A.2 The Calculation for indices of refraction of 1-Bromonaphthalene

1-Bromonaphthalene refractive indices can be treated as according to the Cauchy's equation, (Jenkins and White, 1976).

$$n = A + \frac{B}{\lambda^2} + \frac{C}{\lambda^4}. \quad (\text{A.3})$$

From (A.3), its dependence of wavelength can be utilized to compute the unknown constants A, B and C, which is specific for each medium in order to reveal the refractive indices at  $\lambda = 450$  and  $900$  nm. Therefore, the 4 samples of well-known refractive indices of 1-Bromonaphthalene as shown in table A.2 are exploited to determine the constants A, B and C by using the Cramer's Rule as follows.

$$\begin{bmatrix} n_1 \\ n_2 \\ n_3 \end{bmatrix} = \begin{bmatrix} A_1 & B_1 & C_1 \\ A_2 & B_2 & C_2 \\ A_3 & B_3 & C_3 \end{bmatrix} \begin{bmatrix} 1 \\ 1/\lambda^2 \\ 1/\lambda^4 \end{bmatrix} \quad (\text{A.2})$$

**Table A.2.** Changes in refractive indices of 1-Bromonaphthalene with a wavelength range 0.434-1.064  $\mu\text{m}$ .

$\lambda$ ( $\mu\text{m}$ )	$n_{\text{liq}}$
0.434	1.7041
0.486	1.6817
0.532	1.6701
0.977	1.6340
1.064	1.6262

Therefore, sets of each sample simultaneously lead to determine the RDP refractive indices shown by table A.3.

From tables A.3, the refractive indices of 1-Bronaphthalene at 450 and 900 nm are 1.6952 and 1.6335, respectively, that will be utilized to clarify the reflected second harmonic generation.

**Table A.3.** The sets of samples and calculated RDP refractive indices and its average value

NO.	$I_1(\text{nm})$	$I_2(\text{nm})$	$I_3(\text{nm})$	$n_{liq}$ at 450 nm	$n_{liq}$ at 900 nm
1	1.064	0.532	0.434	1.69669	1.63155
2	0.486	0.532	1.064	1.69350	1.63200
3	1.064	0.977	0.532	1.69408	1.64306
4	0.977	0.532	0.434	1.69643	1.63625
Average refractive indices				1.6952	1.6335



Given the nonlinear polarization,  $\vec{P}_{2w}^{NLS}$ , lies in optical axis of the crystal, z-axis, along plane of incidence as shown by figure B.1.

From the figure,

$$|-\mathbf{q}_T| = \mathbf{q}_T = 90^\circ - \mathbf{b}. \quad (\text{B.1})$$

Using Snell's law,

$$n_{liq}^w \sin \mathbf{q}_i^{NB} = n_e^{2w}(2\mathbf{q}_T) \sin \mathbf{q}_T. \quad (\text{B.2})$$

To find the index of ellipsoid, consider

$$\frac{1}{[n_e^{2w}(2\mathbf{q}_T)]^2} = \frac{\cos^2(2\mathbf{q}_T)}{[n_o^{2w}]^2} + \frac{\sin^2(2\mathbf{q}_T)}{[n_e^{2w}(\mathbf{p}/2)]^2}$$

or

$$\frac{1}{[n_e^{2w}(180^\circ - 2\mathbf{b})]^2} = \frac{\cos^2(180^\circ - 2\mathbf{b})}{[n_o^{2w}]^2} + \frac{\sin^2(180^\circ - 2\mathbf{b})}{[n_e^{2w}(\mathbf{p}/2)]^2}. \quad (\text{B.3})$$

From (B.1), we find that

$$n_e^{2w}(180^\circ - 2\mathbf{b}) = \frac{n_{liq}^w \sin \mathbf{q}_i^{NB}}{\sin(90^\circ - \mathbf{b})}. \quad (\text{B.4})$$

Substituting (B.4)  $\rightarrow$  (B.3),

$$\left[ \frac{\sin(90^\circ - \mathbf{b})}{n_{liq}^w \sin \mathbf{q}_i^{NB}} \right]^2 = \frac{\cos^2(180^\circ - 2\mathbf{b})}{[n_o^{2w}]^2} + \frac{\sin^2(180^\circ - 2\mathbf{b})}{[n_e^{2w}(\mathbf{p}/2)]^2}, \quad (\text{B.5})$$

Yielding  $A = [n_{liq}^w \sin \mathbf{q}_i^{NB}]^2 \quad (\text{B.6.1})$

$$B = [n_o^{2w}]^2 \quad (\text{B.6.2})$$

$$C = [n_e^{2w}(\mathbf{p}/2)]^2 \quad (\text{B.6.3})$$

Substituting

$$\cos(180^\circ - 2\mathbf{b}) = 1 - 2 \sin^2(90^\circ - \mathbf{b})$$

and

$$\sin^2(180^\circ - 2\mathbf{b}) = 4 \sin^2(90^\circ - \mathbf{b}) - 4 \sin^4(90^\circ - \mathbf{b})$$

in (5):

$$BC \sin^2(90^\circ - \mathbf{b}) = AC[1 - 4 \sin^2(90^\circ - \mathbf{b}) + 4 \sin^4(90^\circ - \mathbf{b})] + AB[\sin^2(90^\circ - \mathbf{b}) - 4 \sin^4(90^\circ - \mathbf{b})]$$

Letting  $x = \sin^2(90^\circ - \mathbf{b})$ ,

$$BCx = AC[1 - 4x + 4x^2] + AB[x - 4x^2],$$

or

$$0 = AC - (BC + 4AC - 4AB)x + (4AC - 4AB)x^2. \quad (\text{B.7})$$

Substitute the values of refractive index for constant  $A, B, C$  by

$$n_e^{2w}(\mathbf{p}/2) = 1.4857,$$

$$n_o^{2w} = 1.5160, \text{ and}$$

$$n_{liq}^w = 1.6335,$$

for  $\mathbf{q}_i^{NB} = 30^\circ$

$$[\sin \mathbf{q}_i^{NB}] = 0.5.$$

Therefore, from (6), we get

$$A = 0.66708$$

$$B = 2.29826 \quad \text{and}$$

$$C = 2.20730$$

Solving for (6),

$$x^2 = 0.30030$$

$$x = 0.54800$$

or

$$\sin(90^\circ - \mathbf{b}) = \sin \mathbf{q}_r = 0.54800.$$

Then

$$\mathbf{q}_r = 33.23^\circ$$

and

$$\mathbf{b} = 56.77^\circ.$$

Therefore the Nonlinear Brewster angle will occur at  $\mathbf{q}_i^{NB} = 30^\circ$  when the

$\vec{P}_{2w}^{NLS}$  makes the angle between the crystal surface with  $\mathbf{b} = 56.77^\circ$ . At this  $\vec{P}_{2w}^{NLS}$

orientation, second harmonic generation disappears,  $I_R^{2w} \rightarrow 0$ , which is the Nonlinear Brewster angle condition.

**Checking for the  $\vec{P}_{2w}^{NLS}$  orientation with  $\mathbf{b} = 56.77^\circ$  gives the Nonlinear Brewster angle at  $\mathbf{q}_i^{NB} = 30^\circ$ .**

From Snell's law, (B.2)

$$n_{liq}^w \sin \mathbf{q}_i^{NB} = n_e^{2w}(2\mathbf{q}_T) \sin \mathbf{q}_T, \quad (\text{B.2})$$

then

$$\mathbf{q}_i^{NB} = \sin^{-1} \left[ \frac{n_e^{2w}(2\mathbf{q}_T) \sin \mathbf{q}_T}{n_{liq}^w} \right]. \quad (\text{B.8})$$

For index of ellipsoid,

$$\frac{1}{[n_e^{2w}(2\mathbf{q}_T)]^2} = \frac{\cos^2(2\mathbf{q}_T)}{[n_o^{2w}]^2} + \frac{\sin^2(2\mathbf{q}_T)}{[n_e^{2w}(\mathbf{p}/2)]^2},$$

By substitution of

$$n_e^{2w}(\mathbf{p}/2) = 1.4857,$$

$$n_o^{2w} = 1.5160,$$

$$n_{liq}^w = 1.6335,$$

and

$$\mathbf{q}_T = 33.23^\circ,$$

then

$$n_e^{2w}(2\mathbf{q}_r) = 1.4904.$$

Substitute into (8), and obtain

$$\mathbf{q}_i^{NB} = \sin^{-1} \left[ \frac{1.4904 \sin(33.23^\circ)}{1.6335} \right] = 30^\circ.$$

That confirms previous work.

## APPENDIX C

### COMPUTER PROGRAM

#### C 1. Reflected SHI of RDP Crystal at 900 nm with Nonlinear Polarization 52.93 Degreed Lies with Face Normal

```
#include <iostream.h>

#include <math.h>

#include <iomanip.h>

#include <stdio.h>

#include <conio.h>

#include <complex.h>

complex nee(complex);

double ref(complex,complex);

int show(double, complex, double, int);

complex Oig;

void main()

{

    float AngS, AngE, AngEE, Add;

    complex OiD,OR,Os,OTT,SHI, Degg;
```

```
complex nE2, OT, OTD;

double x=0;

const float nO1w=1.4965;

const float nO2w=1.5160;

const float nE2w=1.4857;

const float nL1w=1.6335;

const float nL2w=1.6952;

const float Pi=3.1415927;

complex O_s, Oi;

clrscr();

FILE *stream;

FILE *index;

stream=fopen("SHI0.txt","w+");

index=fopen("nRDP.txt", "w+");

cout << "\n\nTransmitted Angle: Starting "; cin >> AngS;

cout << "Transmitted Angle: Ending "; cin >> AngE;

cout << "Transmitted Angle : Increasing ";cin >> Add;

cout << endl << setw(10)<< " Inci(deg) ";

cout << setw(12) << " index of RDP";

cout << setw(15) << " Reflected SHI" << endl;

OTD = AngS;

AngEE = AngE;

int i=0;

while(imag(OTD) >= 90-AngEE) {
```

```

OT=OTD*Pi/180;

nE2=nec(OT);

SHI = ref(OT, nE2);

Degg = real(abs(Oig)*180/Pi);

if(real(OTD) < 0) Degg = -Degg;

fprintf(stream, "%6.3lf\t%15.8lg\n", real(Degg), real(SHI));

fprintf(index, "%7.6lf, %7.3lf\n", nE2, Degg);

i = show(real(Degg), nE2, real(SHI), i);

if(real(OTD)<90)

{

    if(real(OTD) == 89) OTD+=0.01;

    else OTD+=Add;

}

else {

    if(imag(OTD) > -1) x-=0.01;

    else x-=Add;

    OTD=complex(90, x);

}

}

fclose(stream);

fclose(index);

cout << "Completely Calculating";

getch();

}

```

```

complex nee(complex OT)
{
    complex O_s,ss, xx;
    const float nL1w = 1.6335;
    const float nO2w = 1.5160;
    const float nE2w = 1.4857;
    const float nO1w = 1.4965;
    const float pii =3.1415927;
    xx=1/sqrt(pow(cos(OT+(90.00-52.93)*pii/180.00),2)/(nO2w*nO2w)+pow(sin
(OOT+(90.00-52.93)*pii/180.00),2)/(nE2w*nE2w));
    complex nE2 = abs(xx);
    return nE2;
}

double ref(complex O_t, complex nE2)
{
    complex tt;
    const float Piii=3.1415927;
    const float nO1w=1.4965;
    const float nL1w=1.6335;
    const float nL2w=1.6952;
    complex ii=nE2*sin(O_t)/nL1w;
    complex Oi=asin(ii);
    Oig = real(Oi);
    Oi = Oig;
}

```

```

complex OR=asin(nL1w*sin(Oi)/nL2w);

complex ss = nL1w*sin(Oi)/nO1w;

complex O_s = asin(ss);

complex crit_w=asin(nO1w/nL1w);

complex FLm =2*cos(Oi)/((sin(crit_w)*cos(O_s))+cos(Oi));

complex
FNLm=(sin(O_s)*sin(O_t)*sin(O_t)*sin(O_t+(270.00+52.93)*Piii/180))/
(sin(OR)*sin(O_t+OR)*cos(O_t-OR)*sin
(O_t+O_s));

double Ir=real(abs(pow(abs(FLm), 4.0)*pow(abs(FNLm), 2.0)*cos(OR)/cos
(Oi)));

return Ir;
}

int show(double Degg, complex nE2, double SHI, int i)
{

printf("%8.3lf |", Degg);

printf("%10.6lf |", real(nE2));

printf("%15.8lg \n",SHI);

if(i>20)
{ i=0;

getch();

}

i++;

return i;}

```

## C 2. Reflected SHI of RDP at 900 nm with Nonlinear Polarization

### Lies in Face Normal

```
#include <iostream.h>

#include <math.h>

#include <iomanip.h>

#include <stdio.h>

#include <conio.h>

#include <complex.h>

complex nee(complex);

double ref(complex,complex);

int show(double, complex, double, int);

complex Oig;

void main()

{

    float AngS, AngE, AngEE, Add;

    complex OiD,OR,Os,OTT,SHI, Degg;

    complex nE2, OT, OTD;

    double x=0;

    const float nO1w=1.4965;

    const float nO2w=1.5160;

    const float nE2w=1.4857;

    const float nL1w=1.6335;

    const float nL2w=1.6952;
```

```

const float Pi=3.1415927;

complex O_s, Oi;

clrscr();

FILE *stream;

FILE *index;

stream=fopen("SHI0.txt","w+");

index=fopen("nRDP.txt", "w+");

cout << "\n\nTransmitted Angle: Starting "; cin >> AngS;

cout << "Transmitted Angle: Ending "; cin >> AngE;

cout << "Transmitted Angle : Increasing ";cin >> Add;

cout << endl << setw(10)<< " Inci(deg) ";

cout << setw(12) << " index of RDP";

cout << setw(15) << " Reflected SHI" << endl;

OTD = AngS;

AngEE = AngE;

int i=0;

while(imag(OTD) >= 90-AngEE) {

    OT=OTD*Pi/180;

    nE2=nec(OT);

    SHI = ref(OT, nE2);

    Degg = real(abs(Oig)*180/Pi);

    if(real(OTD) < 0) Degg = -Degg;

    fprintf(stream, "%6.3lf\t%15.8lg\n", real(Degg), real(SHI));

    fprintf(index, "%7.6lf, %7.3lf\n", nE2, Degg);

```

```

        i = show(real(Degg), nE2, real(SHI), i);
        if(real(OTD)<90)
        {
            if(real(OTD) == 89) OTD+=0.01;
            else OTD+=Add;
        }
        else {
            if(imag(OTD) > -1) x-=0.01;
            else x-=Add;
            OTD=complex(90, x);
        }
    }
    fclose(stream);
    fclose(index);
    cout << "Completely Calculating";
    getch();
}
complex nee(complex OT)
{
    complex O_s,ss, xx;
    const float nL1w = 1.6335;
    const float nO2w = 1.5160;
    const float nE2w = 1.4857;
    const float nO1w = 1.4965;

```

```

const float pii =3.1415927;

xx=1/sqrt(pow(cos(OT),2)/(nO2w*nO2w)+pow(sin(OT),2)/(nE2w*nE2w));

complex nE2 = abs(xx);

return nE2;

}

double ref(complex O_t, complex nE2)

{

    complex tt;

    const float Piii=3.1415927;

    const float nO1w=1.4965;

    const float nL1w=1.6335;

    const float nL2w=1.6952;

    complex ii=nE2*sin(O_t)/nL1w;

    complex Oi=asin(ii);

    Oig = real(Oi);

    Oi = Oig;

    complex OR=asin(nL1w*sin(Oi)/nL2w);

    complex ss = nL1w*sin(Oi)/nO1w;

    complex O_s = asin(ss);

    complex crit_w=asin(nO1w/nL1w);

    complex FLm =2*cos(Oi)/((sin(crit_w)*cos(O_s))+cos(Oi));

    complex FNLm=(sin(O_s)*sin(O_t)*sin(O_t)*sin(O_t)/

(sin(OR)*sin(O_t+OR)*cos(O_t-OR)*sin(O_t+O_s));

```

```

        double Ir=real(abs(pow(abs(FLm), 4.0)*pow(abs(FNLm), 2.0)*cos(OR)/cos
(Oi)));

        return Ir;
    }

int show(double Degg, complex nE2, double SHI, int i)
{
    printf("%8.3lf |", Degg);
    printf("%10.6lf |", real(nE2));
    printf("%15.8lg \n",SHI);
    if(i>20)
    { i=0;
    getch();
    }
    i++;
    return i;
}

```

### **C 3. Reflected SHI of RDP at 900 nm with Nonlinear Polarization 90 Degreed Lies with Face Normal**

```

#include <iostream.h>

#include <math.h>

#include <iomanip.h>

```

```
#include <stdio.h>

#include <conio.h>

#include <complex.h>

complex nee(complex);

double ref(complex,complex);

int show(double, complex, double, int);

complex Oig;

void main()

{

    float AngS, AngE, AngEE, Add;

    complex OiD,OR,Os,OTT,SHI, Degg;

    complex nE2, OT, OTD;

    double x=0;

    const float nO1w=1.4965;

    const float nO2w=1.5160;

    const float nE2w=1.4857;

    const float nL1w=1.6335;

    const float nL2w=1.6952;

    const float Pi=3.1415927;

    complex O_s, Oi;

    clrscr();

    FILE *stream;

    FILE *index;

    stream=fopen("SHI0.txt","w+");
```

```

index=fopen("nADP.txt", "w+");

cout << "\n\nTransmitted Angle: Starting "; cin >> AngS;

cout << "Transmitted Angle: Ending "; cin >> AngE;

cout << "Transmitted Angle : Increasing ";cin >> Add;

cout << endl << setw(10)<< " Inci(deg) ";

cout << setw(12) << " index of RDP";

cout << setw(15) << " Reflected SHI" << endl;

OTD = AngS;

AngEE = AngE;

int i=0;

while(imag(OTD) >= 90-AngEE) {

    OT=OTD*Pi/180;

    nE2=nec(OT);

    SHI = ref(OT, nE2);

    Degg = real(abs(Oig)*180/Pi);

    if(real(OTD) < 0) Degg = -Degg;

    fprintf(stream, "%6.3lf\t%15.8lg\n", real(Degg), real(SHI));

    fprintf(index, "%7.6lf, %7.3lf\n", nE2, Degg);

    i = show(real(Degg), nE2, real(SHI), i);

    if(real(OTD)<90)

    {

        if(real(OTD) == 89) OTD+=0.01;

        else OTD+=Add;

    }

}

```

```

        else {
            if(imag(OTD) > -1) x-=0.01;
            else x-=Add;
            OTD=complex(90, x);
        }
    }

    fclose(stream);
    fclose(index);

    cout << "Completely Calculating";
    getch();
}

complex nee(complex OT)
{
    complex O_s,ss, xx;

    const float nL1w = 1.6335;
    const float nO2w = 1.5160;
    const float nE2w = 1.4857;
    const float nO1w = 1.4965;
    const float pii =3.1415927;

    xx=1/sqrt(pow(cos(OT+(90.00)*pii/180.00),2)/(nO2w*nO2w)+pow(sin(OT+(90.00)*pii/180.00),2)/(nE2w*nE2w));

    complex nE2 = abs(xx);
    return nE2;
}

```

```

double ref(complex O_t, complex nE2)
{
    complex tt;

    const float Piii=3.1415927;

    const float nO1w=1.4965;

    const float nL1w=1.6335;

    const float nL2w=1.6952;

    complex ii=nE2*sin(O_t)/nL1w;

    complex Oi=asin(ii);

    Oig = real(Oi);

    Oi = Oig;

    complex OR=asin(nL1w*sin(Oi)/nL2w);

    complex ss = nL1w*sin(Oi)/nO1w;

    complex O_s = asin(ss);

    complex crit_w=asin(nO1w/nL1w);

    complex FLm =2*cos(Oi)/((sin(crit_w)*cos(O_s))+cos(Oi));

    complex

FNLm=(sin(O_s)*sin(O_t)*sin(O_t)*sin(O_t+(270.00+0.00)*Piii/180))/

    (sin(OR)*sin(O_t+OR)*cos(O_t-OR)*sin(O_t+O_s));

    double Ir=real(abs(pow(abs(FLm), 4.0)*pow(abs(FNLm), 2.0)*cos(OR)/cos

(Oi)));

    return Ir;

}

```

```

int show(double Degg, complex nE2, double SHI, int i)
{
    printf("%8.3lf |", Degg);
    printf("%10.6lf |", real(nE2));
    printf("%15.8lg \n",SHI);
    if(i>20)
    { i=0;
      getch();
    }
    i++;
    return i;
}

```

#### **C 4. Reflected SHI of RDP Crystal at 900 nm with Nonlinear Polarization 56.77 Degreeed Lies with Face Normal**

```

#include <iostream.h>

#include <math.h>

#include <iomanip.h>

#include <stdio.h>

#include <conio.h>

#include <complex.h>

complex nee(complex);

double ref(complex,complex);

```

```

int show(double, complex, double, int);

complex Oig;

void main()
{
    float AngS, AngE, AngEE, Add;

    complex OiD,OR,Os,OTT,SHI, Degg;

    complex nE2, OT, OTD;

    double x=0;

    const float nO1w=1.4965;

    const float nO2w=1.5160;

    const float nE2w=1.4857;

    const float nL1w=1.6335;

    const float nL2w=1.6952;

    const float Pi=3.1415927;

    complex O_s, Oi;

    clrscr();

    FILE *stream;

    FILE *index;

    stream=fopen("SHI0.txt","w+");

    index=fopen("nRDP.txt", "w+");

    cout << "\n\nTransmitted Angle: Starting "; cin >> AngS;

    cout << "Transmitted Angle: Ending "; cin >> AngE;

    cout << "Transmitted Angle : Increasing ";cin >> Add;

    cout << endl << setw(10)<< " Inci(deg) ";

```

```

cout << setw(12) << " index of RDP";

cout << setw(15) << " Reflected SHI" << endl;

OTD = AngS;

AngEE = AngE;

int i=0;

while(imag(OTD) >= 90-AngEE) {

    OT=OTD*Pi/180;

    nE2=nec(OT);

    SHI = ref(OT, nE2);

    Degg = real(abs(Oig)*180/Pi);

    if(real(OTD) < 0) Degg = -Degg;

    fprintf(stream, "%6.3lf\t%15.8lg\n", real(Degg), real(SHI));

    fprintf(index, "%7.6lf, %7.3lf\n", nE2, Degg);

    i = show(real(Degg), nE2, real(SHI), i);

    if(real(OTD)<90)

    {

        if(real(OTD) == 89) OTD+=0.01;

        else OTD+=Add;

    }

    else {

        if(imag(OTD) > -1) x-=0.01;

        else x-=Add;

        OTD=complex(90, x);

    }
}

```

```

    }

    fclose(stream);

    fclose(index);

    cout << "Completely Calculating";

    getch();
}

complex nee(complex OT)
{
    complex O_s,ss, xx;

    const float nL1w = 1.6335;

    const float nO2w = 1.5160;

    const float nE2w = 1.4857;

    const float nO1w = 1.4965;

    const float pii =3.1415927;

    xx=1/sqrt(pow(cos(OT+(90.00-56.77)*pii/180.00),2)/(nO2w*nO2w)+pow(sin
(OT+(90.00-56.77)*pii/180.00),2)/(nE2w*nE2w));

    complex nE2 = abs(xx);

    return nE2;
}

double ref(complex O_t, complex nE2)
{
    complex tt;

    const float Piii=3.1415927;

    const float nO1w=1.4965;

```

```

const float nL1w=1.6335;

const float nL2w=1.6952;

complex ii=nE2*sin(O_t)/nL1w;

complex Oi=asin(ii);

Oig = real(Oi);

Oi = Oig;

complex OR=asin(nL1w*sin(Oi)/nL2w);

complex ss = nL1w*sin(Oi)/nO1w;

complex O_s = asin(ss);

complex crit_w=asin(nO1w/nL1w);

complex FLm =2*cos(Oi)/((sin(crit_w)*cos(O_s))+cos(Oi));

complex

FNLm=(sin(O_s)*sin(O_t)*sin(O_t)*sin(O_t+(270.00+56.77)*Piii/180))/

(sin(OR)*sin(O_t+OR)*cos(O_t-OR)*sin(O_t+O_s));

double Ir=real(abs(pow(abs(FLm), 4.0)*pow(abs(FNLm), 2.0)*cos(OR)/cos

(Oi)));

return Ir;

}

int show(double Degg, complex nE2, double SHI, int i)

{

printf("%8.3lf |", Degg);

printf("%10.6lf |", real(nE2));

printf("%15.8lg \n",SHI);

```

```
if(i>20)
{
    i=0;
    getch();
}
i++;
return i;}
```

## BIOGRAPHY

Miss Manunporn Wongkumdee was born in 1977. She graduated with High School diploma from Suranaree Witthaya School. In 1999 she graduated with a Bachelor's Degree in Telecommunication Engineering with second-class honors at Suranaree University of Technology, Nakhon Ratchasima . Miss Manunporn Wongkumdee was awarded a certificate for her outstanding student activity participation from SUT during her four years of studies and won a scholarship from Shitnawattra Company Group as well as the Nakhon Ratchasima Teacher Cooperative for her ungraduate study. After receiving her Bachelor's Degree, she continued her study in School of Laser Technology and Photonics, Institute of Science at SUT in the Masters Degree Program. During her study she was also awarded a Teaching Assistantship.